

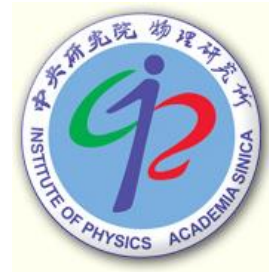


Pion and Kaon PDFs from Drell-Yan and J/Psi Production

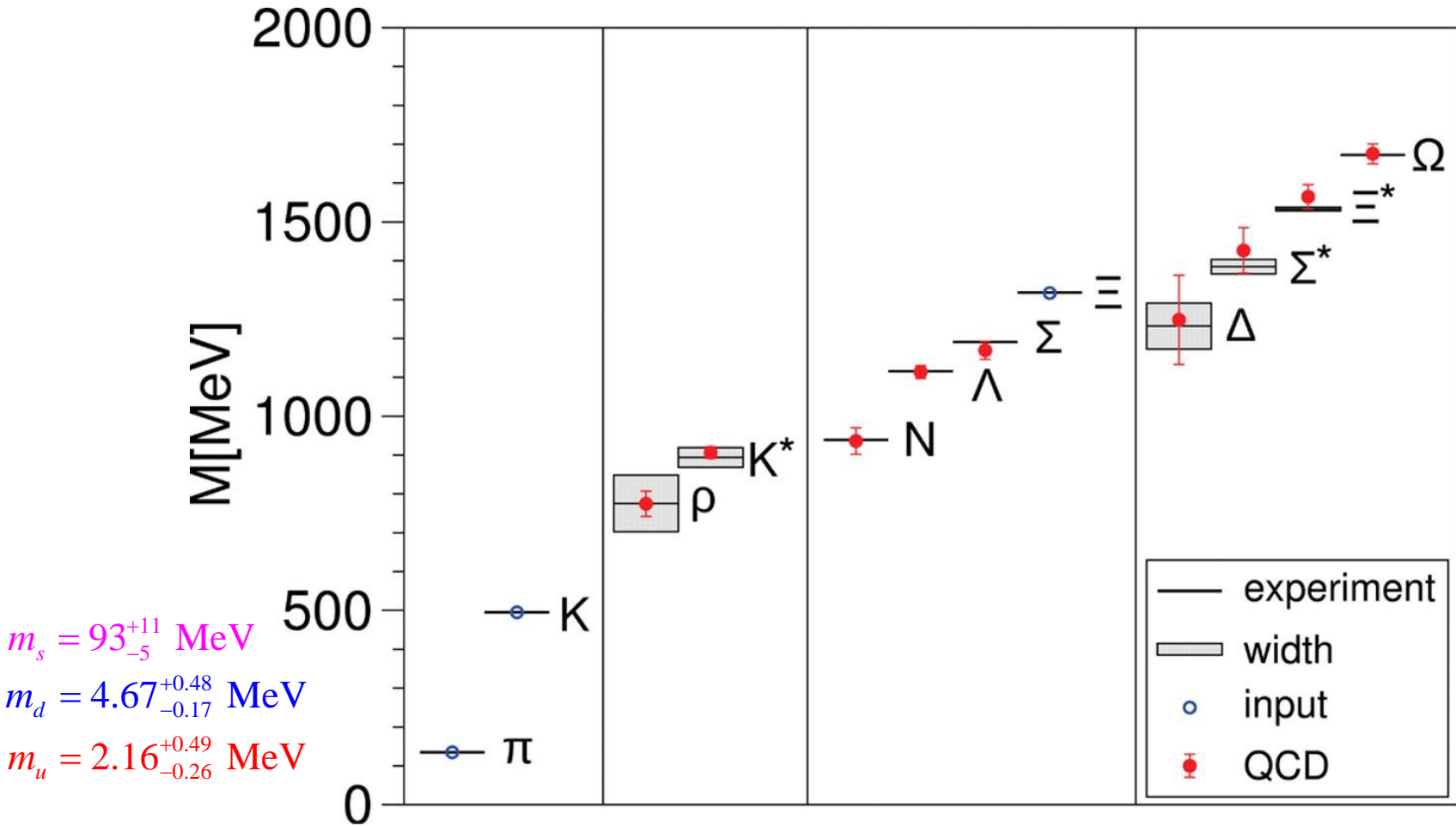
Wen-Chen Chang

Institute of Physics, Academia Sinica

In collaboration with
Chia-Yu Hsieh, Yu-Shiang Lian, Jen-Chieh Peng,
Stephane Platchkov and Takahiro Sawada



Light Hadron Mass Spectrum



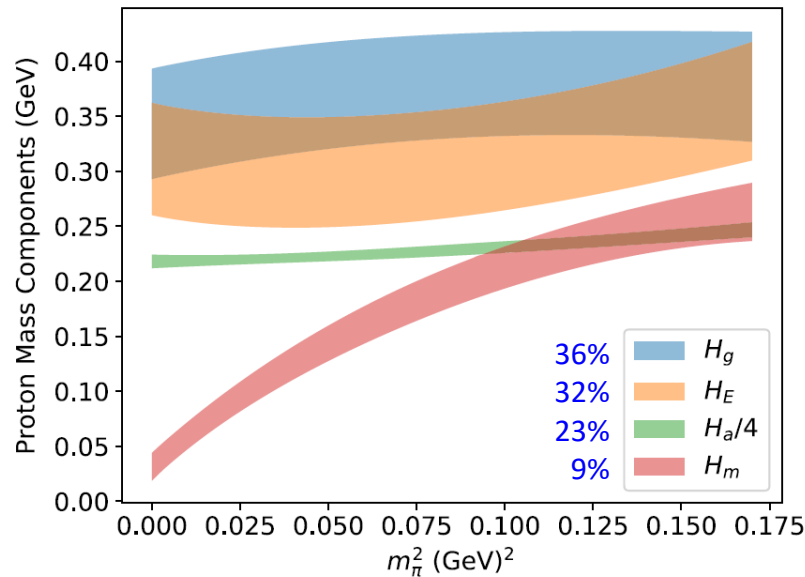
Science 21 November 2008: Vol. 322. no. 5905, pp. 1224 - 1227

DOI: 10.1126/science.1163233 , <http://arxiv.org/pdf/0906.3599v1.pdf>

Mass Decomposition of Proton and Pion from Lattice

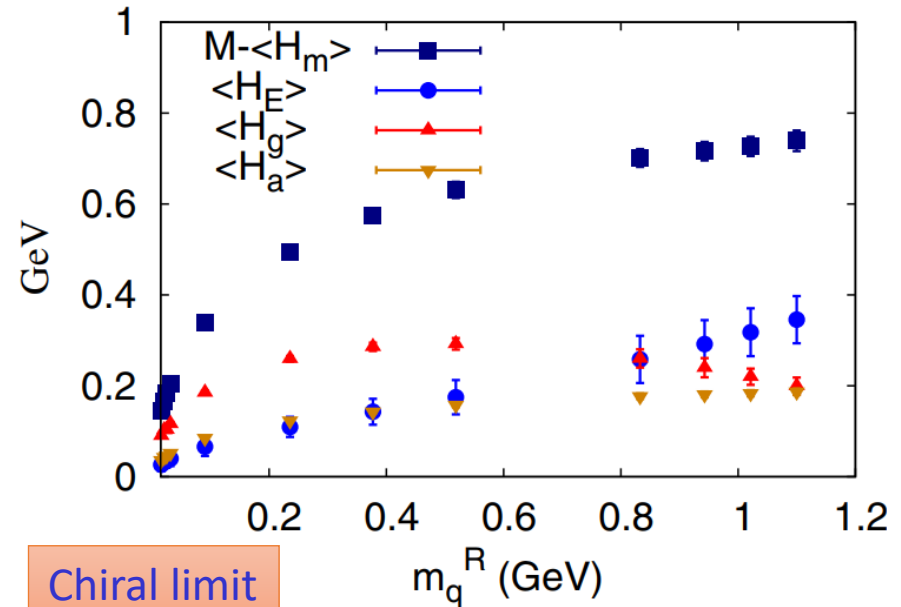
Proton

PRL 121, 212001 (2018)



Pion

PRD 91, 074516 (2015)



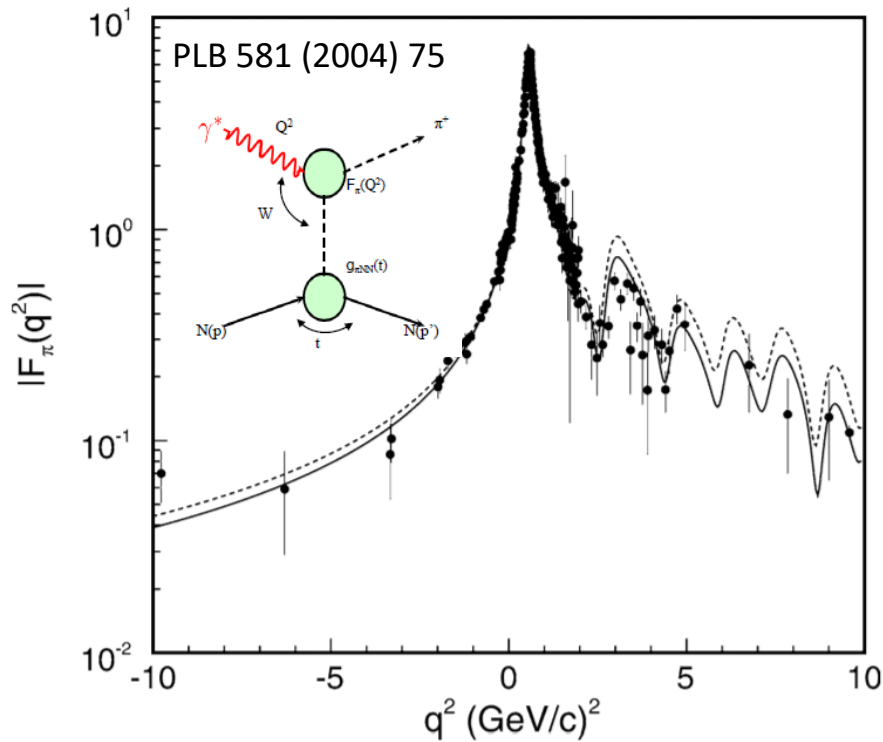
Quark energy

Trace Anomaly (gluon condensate)

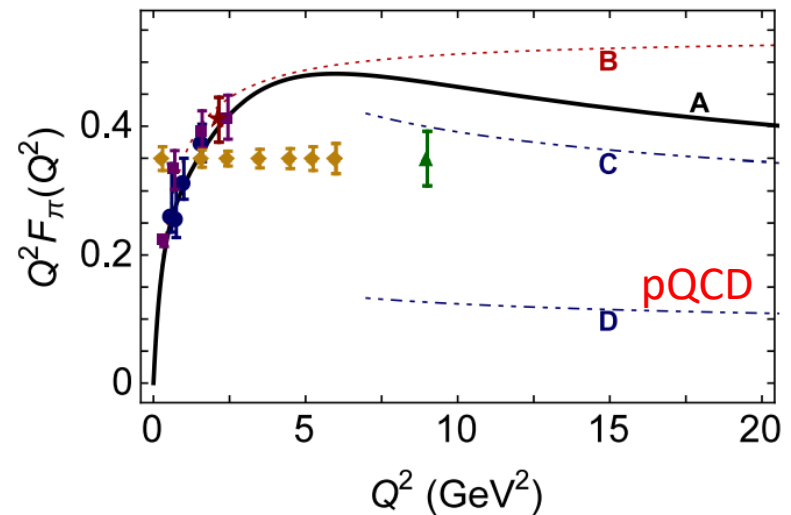
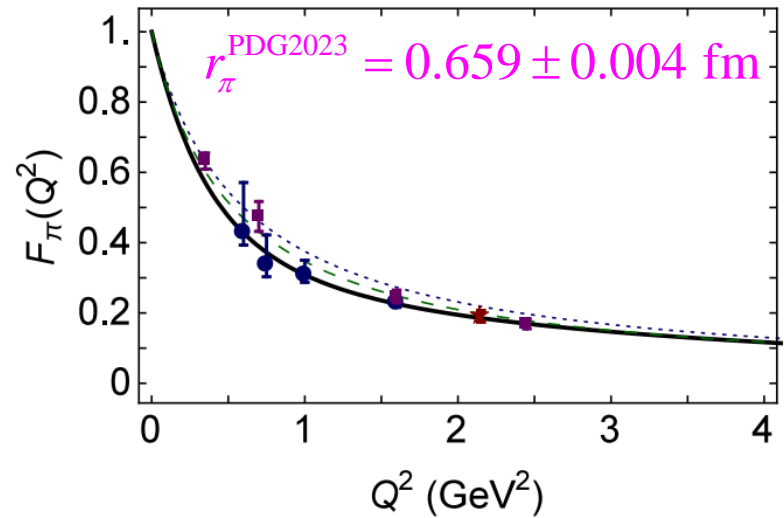
$$M = -\langle T_{44} \rangle = \underbrace{\langle H_m \rangle}_{\text{Quark mass}} + \underbrace{\langle H_E \rangle}_{\text{Gluon energy}}(\mu) + \underbrace{\langle H_g \rangle}_{\text{Gluon energy}}(\mu) + \frac{1}{4} \underbrace{\langle H_a \rangle}_{\text{Trace Anomaly (gluon condensate)}}$$

Form Factors of Pion

Tanja Horn's Talk

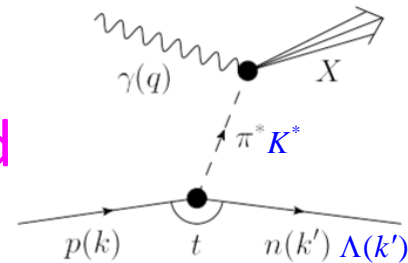


<https://arxiv.org/abs/1602.04016>



Pion/Kaon PDFs

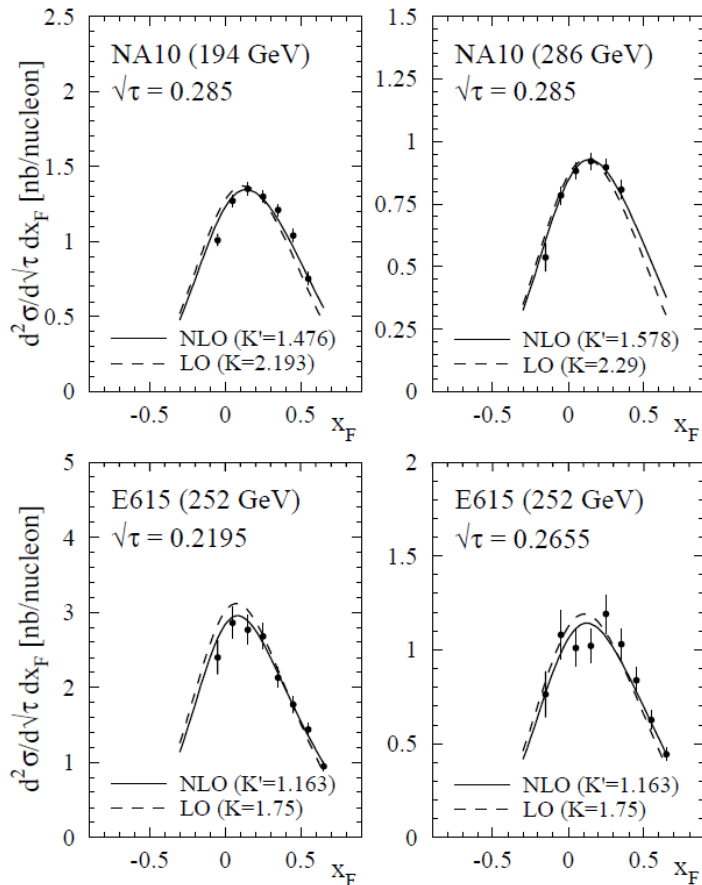
- Drell-Yan: $\pi, K^\pm p \rightarrow \mu^+ \mu^- X$ (LO: sensitive to valence quarks)
 - LO: $q\bar{q} \rightarrow \mu^+ \mu^-$
 - NLO: $q\bar{q} \rightarrow \mu^+ \mu^- G, qG \rightarrow \mu^+ \mu^- q$ (large p_T)
 - NNLO: $q\bar{q}G \rightarrow \mu^+ \mu^- G, qG \rightarrow \mu^+ \mu^- qG, GG \rightarrow \mu^+ \mu^- q\bar{q}$
- Direct photon: $\pi, K^\pm p \rightarrow \gamma X$ (LO: sensitive to gluons)
 - LO: $q\bar{q} \rightarrow \gamma G, qG \rightarrow \gamma q$
- Jpsi: $\pi, K^\pm p \rightarrow J/\psi X$ (LO: sensitive to gluons)
 - LO: $q\bar{q} \rightarrow c\bar{c} \rightarrow J/\psi X, GG \rightarrow c\bar{c} \rightarrow J/\psi X$
 - NLO: $q\bar{q} \rightarrow c\bar{c}G \rightarrow J/\psi X, GG \rightarrow c\bar{c}G \rightarrow J/\psi X, qG \rightarrow c\bar{c}q \rightarrow J/\psi X$
- Leading neutron (LN) electroproduction:
Sullivan processes from a nucleon's pion cloud



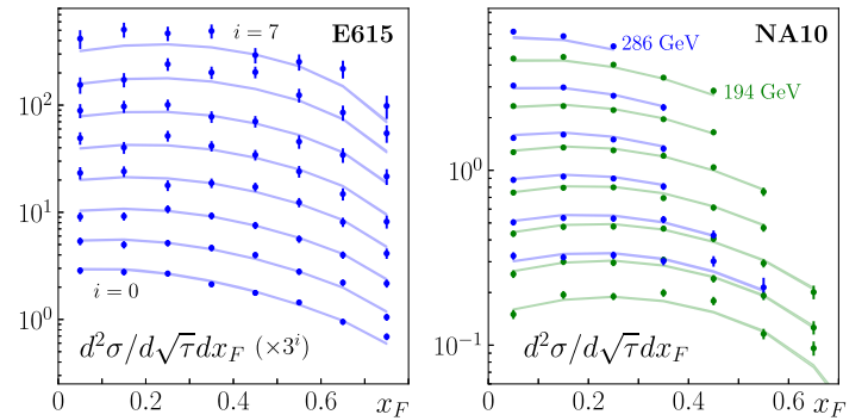
Pion PDFs

Pion-induced Drell-Yan

GRS, [EPJC 1998](#)



JAM, [PRL 2018](#)



NA10 (194 GeV), [ZPC 1985](#)

NA10 (286 GeV), [IMPA 1990](#)

E615 (252 GeV), [PRD 1989](#)

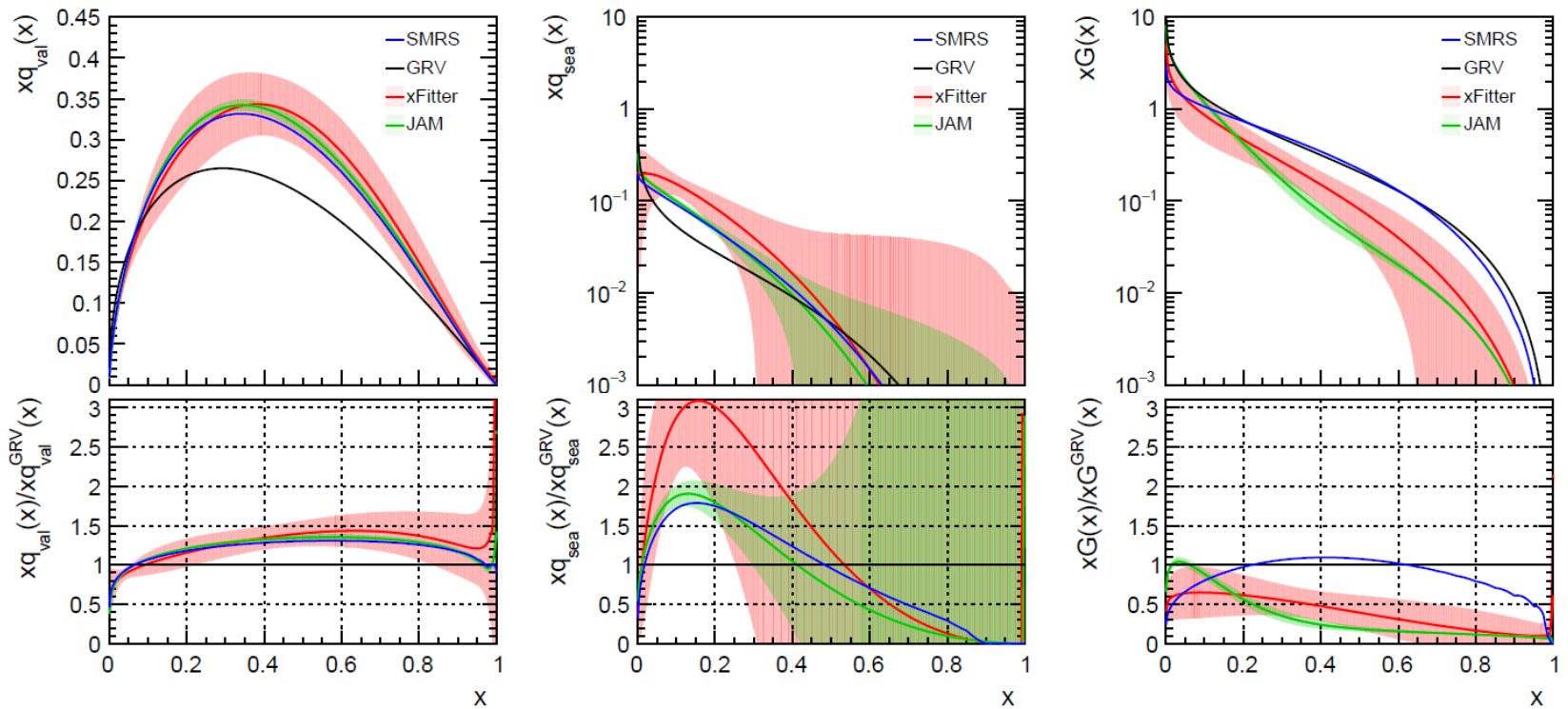
Pion PDFs (2021)

PDF	DY (xF, pT)	Direct γ	J/ψ	LN	Refs.
OW	*		*		PRD 1984
ABFKW	*	*			PLB 1989
SMRS	*	*			PRD 1992
GRV	*	*			ZPC 1992
GRS	*				EPJC 1999
JAM18	*			*	PRL 2018
BS, BBP	*				NPA 2019 PLB 2021
xFitter	*	*			PRD 2020
JAM21	*			*	PRD 2021 PRL 2021

Pion PDFs

$$Q^2 = 9.6 \text{ GeV}^2$$

PDF	$\int_0^1 x \bar{u}_{\text{val}}(x) dx$	$\int_0^1 x \bar{u}_{\text{sea}}(x) dx$	$\int_0^1 x G(x) dx$
OW	0.203	0.026	0.487
ABFKW	0.205	0.026	0.468
SMRS	0.245	0.026	0.394
GRV	0.199	0.020	0.513
JAM ^a	0.225 ± 0.003	0.028 ± 0.002	0.365 ± 0.016
xFitter ^a	0.228 ± 0.009	0.040 ± 0.020	0.291 ± 0.119



A large discrepancy of pion PDFs!

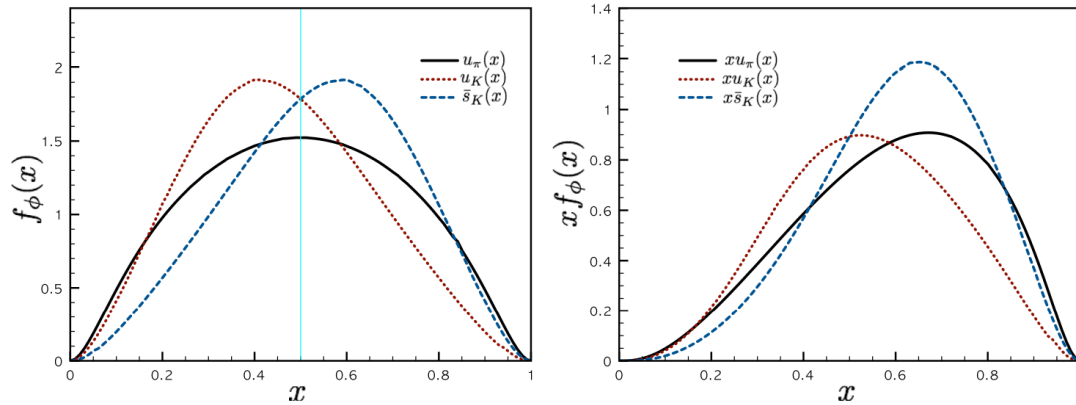
Theoretical Models of Pion/Kaon PDFs

Craig Roberts's Talk
Lorenzo Ross's Talk

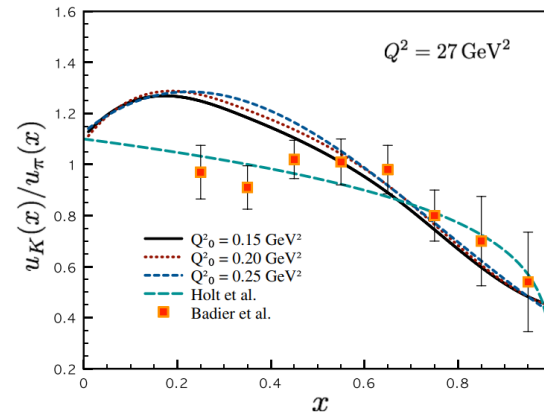
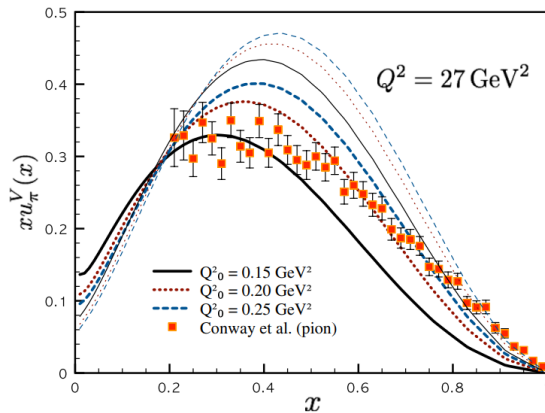
- **Nambu–Jona-Lasinio (NJL) model:** PRC 94, 035201 (2016); PRD 105, 034021, (2022)
- **Chiral constituent quark model:** PRD 86, 074005 (2012); PRD 97, 074015 (2018); 2302.05566 (many were contributed by Seung-il Nam)
- **Dyson-Schwinger Equations (DSE):** PRD 93, 074021 (2016); PRD 93, 054029 (2018); PRL 124, 042002 (2020); EPJC (2020) 80:1064
- **Light-front & Holographic QCD:** PRD 101, 034024 (2020); PRD 106, 034003 (2022); 2303.01789
- **Maximum Entropy Input:** EPJC (2021) 81:302

Parton-distribution functions for the pion and kaon in the gauge-invariant nonlocal chiral-quark model [Seung-il Nam, PRD 86, 074005 (2012)]

Model constructed at an initial scale Q_0



DGLAP QCD evolution

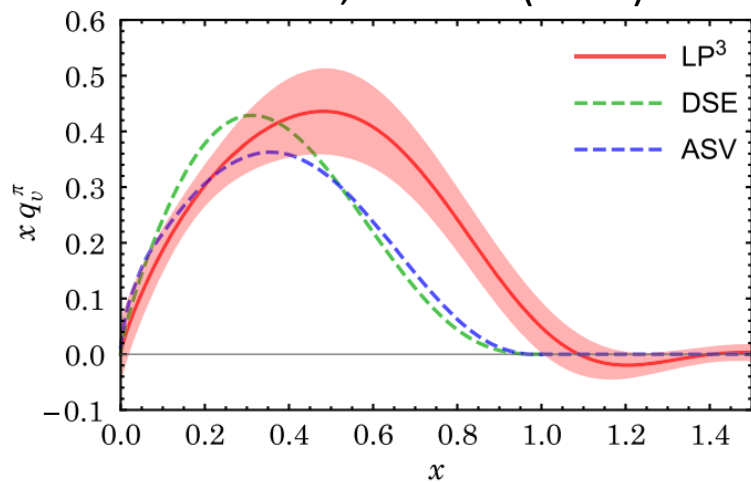


LQCD: Valence & Gluon

Huey-Wen Lin's Talk

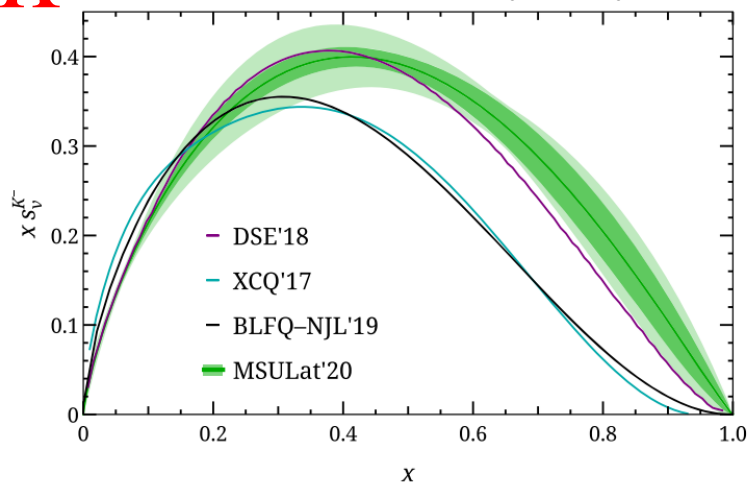
π

PRD 100, 034505 (2019)

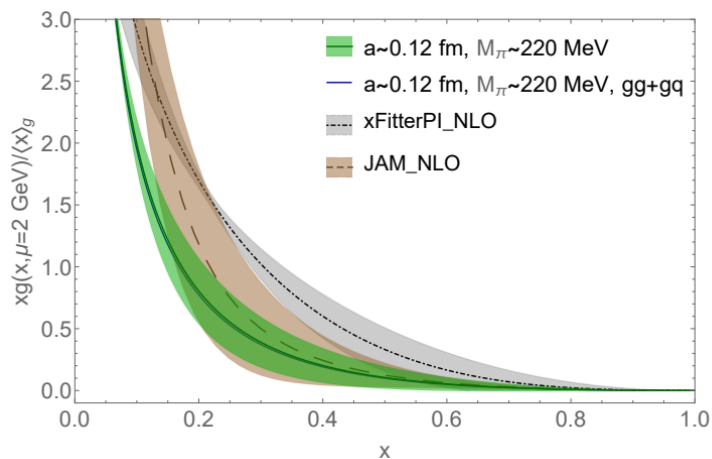


K

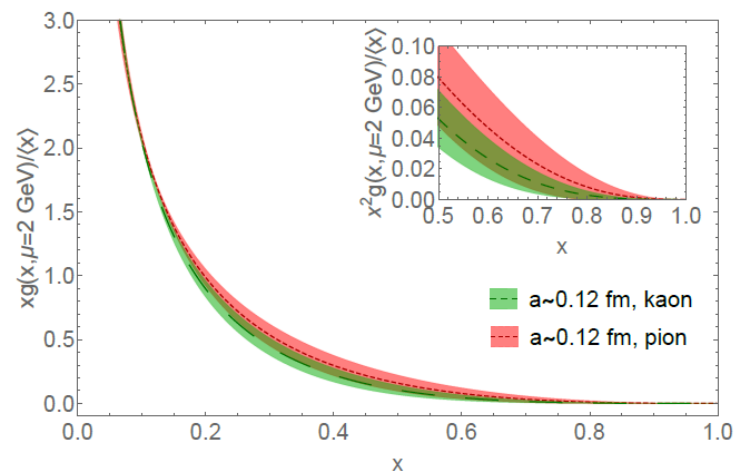
PRD 103, 014516 (2021)



PLB 823, 136778 (2021)

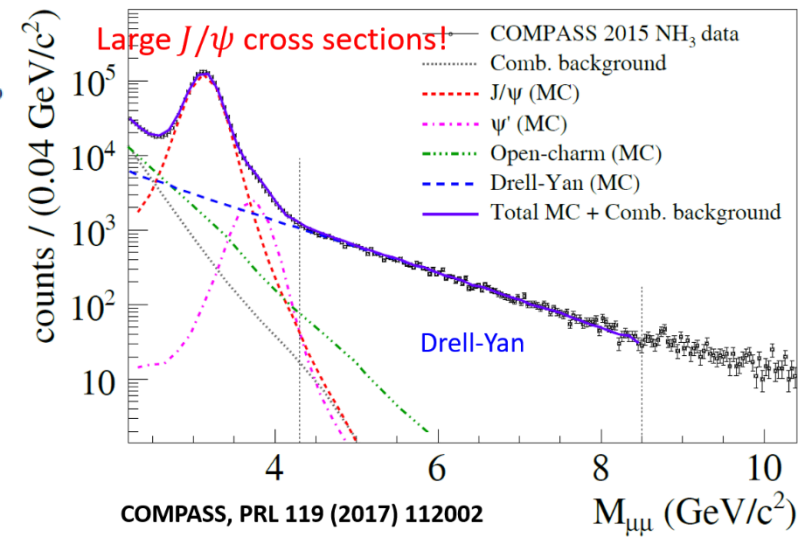


PRD 106, 094510 (2022)



Pion-induced J/psi Production - Fixed-target Experiments

Paper	Reference	Year	Collab	E sqrt(s) (GeV) (GeV)		Beam	Targets
Fermilab							
Branson	PRL 23, 1331	1977	Princ-Chicago	225	20.5	π^- , π^+ , p	C, Sn
Anderson	PRL 42, 944	1979	E444	225	20.5	π^- , π^+ , K^+ , p, ap	C, Cu, W
Abramov	Fermi 91-062-E	1991	E672/E706	530	31.5	π^-	Be
Kartik	PRD 41, 1	1990	E672	530	31.5	π^-	C, AL, Cu, Pb
Katsanevas	PRL 60, 2121	1988	E537	125	15.3	π^- , ap	Be, Cu, W
Akerlof	PR D48, 5067	1993	E537	125	15.3	π^- , ap	Be, Cu, W
Antoniazzi	PRD 46, 4828	1992	E705	300	23.7	π^- , π^+	Li
Gribushin	PR D53, 4723	1995	E672/E706	515	31.1	π^-	Be
Koreshev	PRL 77, 4294	1996	E706/E672	515	31.1	π^-	Be
CERN							
Abolins	PLB 82, 145	1979	WA11/Goliath	150	16.8	π^-	Be
McEwen	PLB 121, 198	1983	WA11	190	18.9	π^-	Be
Badier	Z.Phys. C20, 101	1983	NA3	150	16.8	π^- , π^+ , K^- , K^+ , p, ap	H, Pt
"	"	1983	NA3	200	19.4	π^- , π^+ , K^- , K^+ , p, ap	H, Pt
"	"	1983	NA3	280	22.9	π^- , π^+ , K^- , K^+ , p, ap	H, Pt
Corden	PLB 68, 96	1977	WA39	39.5	8.6	π^- , π^+ , K^- , K^+ , p, ap	Cu
Corden	PLB 96, 411	1980	WA39	39.5	8.6	π^- , π^+ , K^- , K^+ , p, ap	W
Corden	PLB 98, 220	1981	WA39	39.5	8.6	π^- , π^+ , K^- , K^+ , p, ap	p
Corden	PLB 110, 415	1982	WA40	39.5	8.6	π^- , π^+ , K^- , K^+ , p, ap	p, W
Alexandrov	NPB 557, 3	1999	Beatrice	350	25.6	π^-	Si, C, W



LO & NLO Diagrams of $c\bar{c}$ Production

LO

NLO

A. Petrelli et al./Nuclear Physics B 514 (1998) 245–309

A. Petrelli et al./Nuclear Physics B 514 (1998) 245–309

287

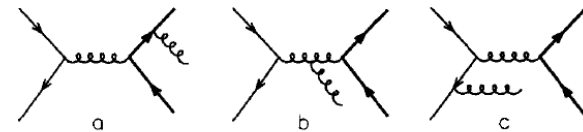
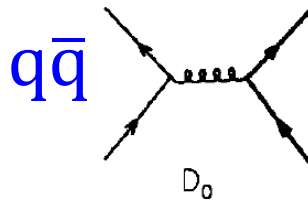
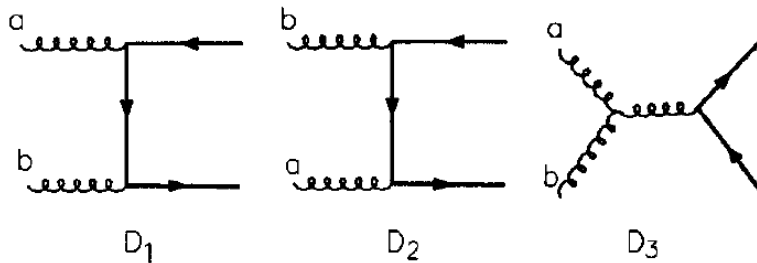


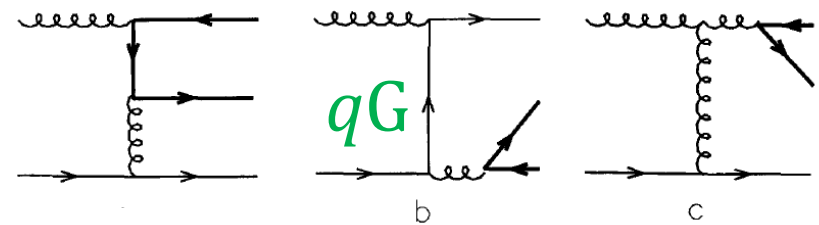
Fig. 8. Diagrams for the real corrections to the $q\bar{q}$ channels. Permutations of outgoing gluons and/or reversal of fermion lines are always implied.

GG



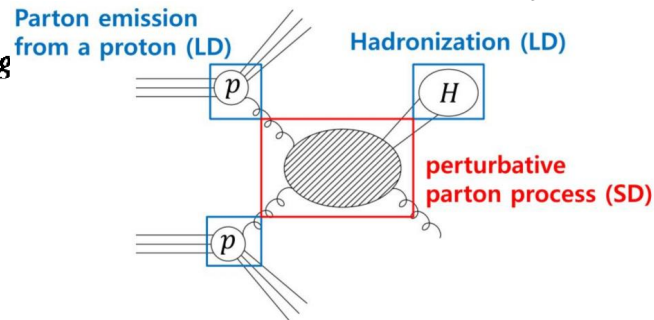
286

A. Petrelli et al./Nuclear Physics B 514 (1998) 245–309



the gq channels. Reversal of fermion lines is always implied.

Fig. 2. Diagrams for the $q\bar{q}$ and g



Color Evaporation Model

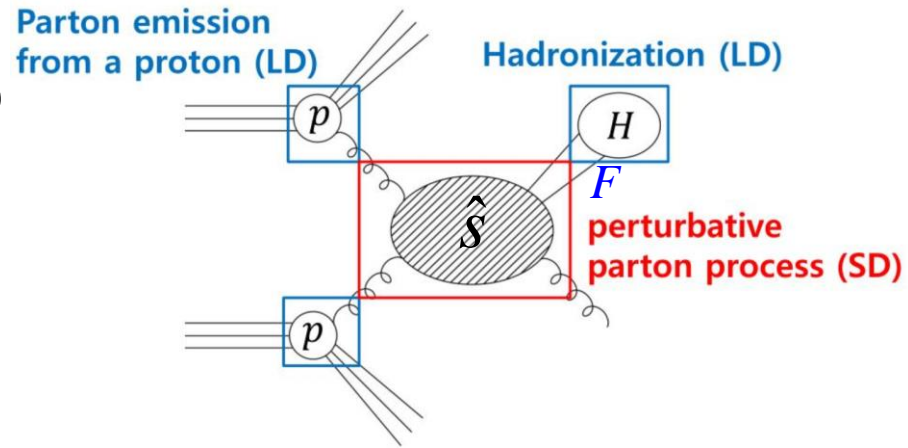
$$\sigma[AB \rightarrow J / \psi X]$$

$$= F \sum_{i,j} \int_{2m_c}^{2m_D} d\hat{s} \int dx_1 dx_2 f_{i/A}(x_1, \mu_F) f_{j/B}(x_2, \mu_F)$$

$$\hat{\sigma}[ij \rightarrow c\bar{c}X](x_1 P_A, x_2 P_B, \mu_F, \mu_R) \delta(\hat{s} - x_1 x_2 s)$$

$$\begin{aligned} \left. \frac{d\sigma}{dx_F} \right|_{J/\psi} &= F \sum_{i,j=q,\bar{q},G} \int_{2m_c}^{2m_D} dM_{c\bar{c}} \frac{2M_{c\bar{c}}}{s \sqrt{x_F^2 + 4M_{c\bar{c}}^2/s}} \\ &\times f_i^\pi(x_1, \mu_F) f_j^N(x_2, \mu_F) \\ &\times \hat{\sigma}[ij \rightarrow c\bar{c}X](x_1 P_\pi, x_2 P_N, \mu_F, \mu_R), \end{aligned}$$

$$x_F = 2p_L/\sqrt{s}, \quad x_{1,2} = \frac{\sqrt{x_F^2 + 4M_{c\bar{c}}^2/s} \pm x_F}{2},$$



LO/NLO calculations of $\hat{\sigma}[ij \rightarrow c\bar{c}X]$:

- P.Nason, S. Dawson and R.K. Ellis, Nucl. Phys. B303 (1988) 607
- M.L. Mangano, P. Nason and G. Ridolfi, Nucl. Phys. B405 (1993) 507

Color evaporation model (CEM)

Phys. Rev. D 102, 054024 (2020); arXiv: 2006.06947

PHYSICAL REVIEW D **102**, 054024 (2020)

Constraining gluon density of pions at large x by pion-induced J/ψ production

Wen-Chen Chang 

Institute of Physics, Academia Sinica, Taipei 11529, Taiwan

Jen-Chieh Peng

Department of Physics, University of Illinois at Urbana-Champaign, Urbana, Illinois 61801, USA

Stephane Platchkov 

IRFU, CEA, Université Paris-Saclay, 91191 Gif-sur-Yvette, France

Takahiro Sawada 

Department of Physics, Osaka City University, Osaka 558-8585, Japan

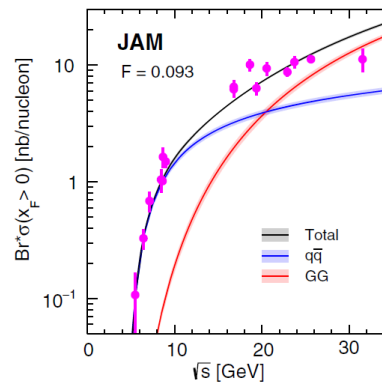
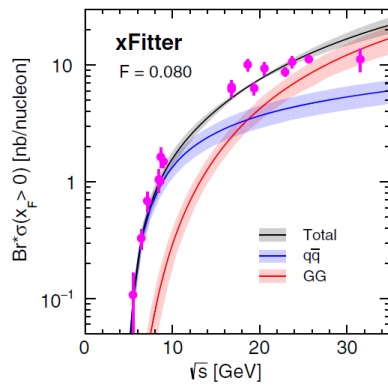
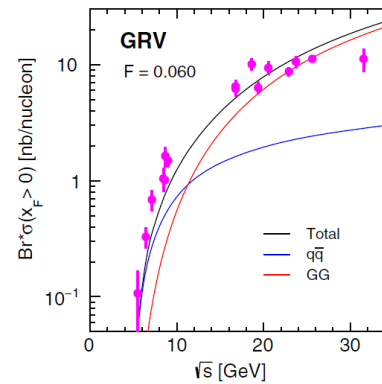
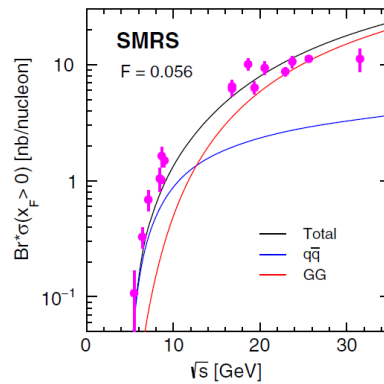


(Received 12 June 2020; accepted 8 September 2020; published 24 September 2020)

The gluon distributions of the pion obtained from various global fits exhibit large variations among them. Within the framework of the color evaporation model, we show that the existing pion-induced J/ψ

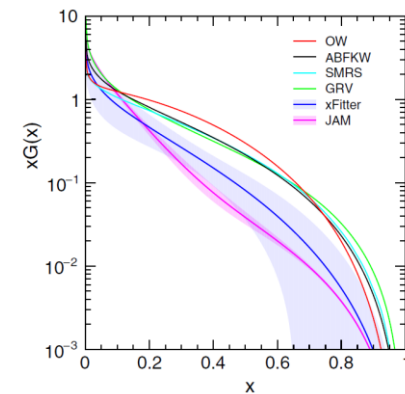
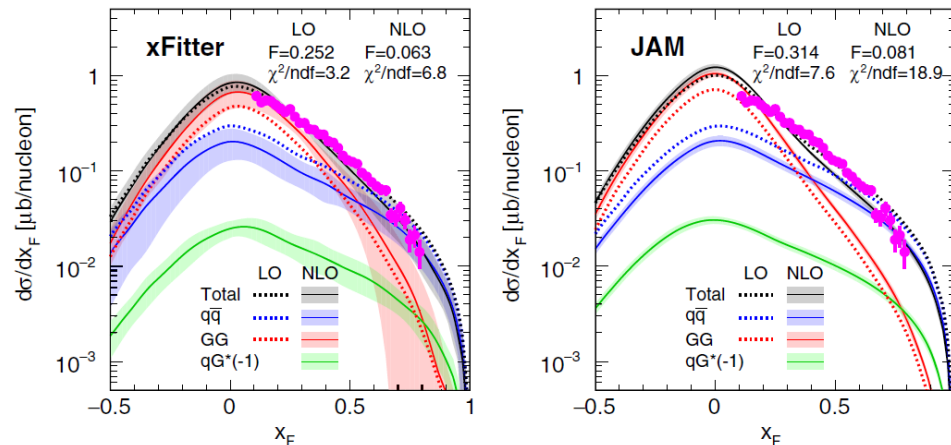
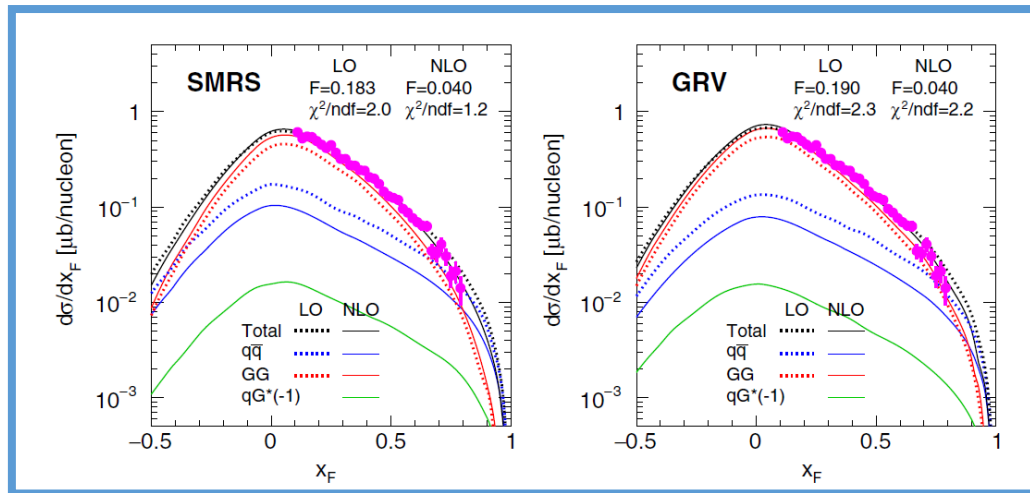
Data vs. CEM NLO: $\sigma(\sqrt{s})$

$$\pi^- + N \rightarrow J\psi + X$$



Data vs. CEM NLO

$[\pi^- + Be \rightarrow J\psi + X \text{ at } 515 \text{ GeV, PRD 53, 4723 (1996)}]$



Data favor SMRS and GRV PDFs with larger gluon densities at $x > 0.1$.

Data vs. CEM Calculations

TABLE III. Results of F factor and χ^2/ndf value of the best fit of the NLO CEM calculations for SMRS, GRV, xFitter, and JAM pion PDFs to the data listed in Table II. The F^* factor and χ^2/ndf^* are the ones corresponding to the fit with inclusion of PDF uncertainties for xFitter and JAM.

Data Experiment (P_{beam})	SMRS		GRV		xFitter				JAM			
	F	χ^2/ndf	F	χ^2/ndf	F	F^*	χ^2/ndf	χ^2/ndf^*	F	F^*	χ^2/ndf	χ^2/ndf^*
E672, E706 (515)	0.040	1.2	0.040	2.2	0.063	0.063	6.8	4.7	0.081	0.081	18.9	18.5
E705 (300)	0.052	2.3	0.053	1.9	0.073	0.076	3.2	1.3	0.086	0.086	16.1	15.9
NA3 (280)	0.046	1.5	0.049	2.0	0.067	0.069	5.0	3.2	0.081	0.081	10.4	10.3
NA3 (200)	0.046	2.1	0.050	2.2	0.065	0.066	5.0	1.3	0.081	0.081	7.7	7.6
WA11 (190)	0.054	5.0	0.058	7.2	0.078	0.076	19.4	6.2	0.091	0.091	73.7	72.9
NA3 (150)	0.065	1.1	0.071	1.0	0.089	0.091	2.6	1.6	0.108	0.108	3.9	3.8
E537 (125)	0.044	1.5	0.049	1.5	0.065	0.065	3.1	1.4	0.083	0.083	3.5	3.5
WA39 (39.5)	0.068	1.3	0.079	1.4	0.073	0.072	1.1	0.8	0.080	0.080	1.2	1.2

- The hadronization factor F is stable across energy.
- High-energy J/ψ data have a large sensitivity to the large- x gluon density of pions.
- The valence-quark distributions plays a minor role if away from the threshold.
- **CEM NLO calculations favor SMRS and GRV PDFs whose gluon densities at $x > 0.1$ are higher, compared with xFitter and JAM PDFs.**

Are these observations model dependent?

NRQCD

The “cascade” (*factorization*) approach of NRQCD

For **heavy** quarkonia
two distinguishable steps
are foreseen

1) **short-distance**
partonic process

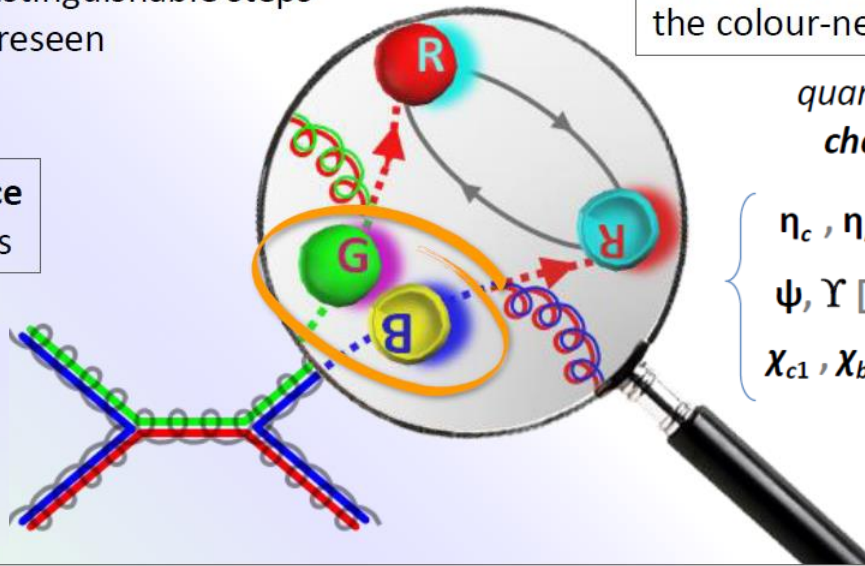
2) **long-distance** evolution to
the colour-neutral bound state

quantum numbers
change to final

$$\left\{ \begin{array}{ll} \eta_c, \eta_b [^1S_0] \\ \psi, \Upsilon [^3S_1] & \chi_{c0}, \chi_{b0} [^3P_0] \\ \chi_{c1}, \chi_{b1} [^3P_1] & \chi_{c2}, \chi_{b2} [^3P_2] \end{array} \right.$$

produces *in general* a coloured $Q\bar{Q}$ pair
of any $^{2S+1}L_J$ quantum numbers

$$\begin{array}{cccc} 1S_0 & 1S_0 & 3S_1 & 3P_0 & 3P_2 \\ & 1D_2 & 3P_2 & 3D_3 & 1P_1 & 3S_1 \\ 3P_1 & & 3D_2 & 3D_1 & 3P_1 \end{array}$$



1) *short-distance coefficients (SDCs)*:
 p_T -dependent partonic cross sections

2) *long-distance matrix elements (LDMEs)*:
constant, **fitted from data**

$$\sigma(A + B \rightarrow Q + X) = \sum_{S, L, C} \mathcal{S}\{A + B \rightarrow (Q\bar{Q})_C [^{2S+1}L_J] + X\} \cdot \mathcal{A}\{(Q\bar{Q})_C [^{2S+1}L_J] \rightarrow Q\}$$

$Q\bar{Q}$ **angular momentum**
and **colour** configurations

NRQCD Framework

PRD 54, 2005 (1996)

PHYSICAL REVIEW D

VOLUME 54, NUMBER 3

1 AUGUST 1996

Hadroproduction of quarkonium in fixed-target experiments

M. Beneke

Stanford Linear Accelerator Center, Stanford University, Stanford, California 94309

I. Z. Rothstein

University of California, San Diego, 9500 Gilman Drive, La Jolla, California 92093

(Received 25 March 1996)

We analyze charmonium and bottomonium production at fixed-target experiments. We find that the inclusion of color octet production channels removes large discrepancies between experiment and the predictions of the color singlet model for the total production cross section. Furthermore, including octet contributions accounts for the observed direct to total J/ψ production ratio. As found earlier for photoproduction of quarkonia, a fit to fixed-target data requires smaller color octet matrix elements than those extracted from high- p_T production at the Fermilab Tevatron. We argue that this difference can be explained by systematic differences in the velocity expansion for collider and fixed-target predictions. While the color octet mechanism thus appears to be an essential part of a satisfactory description of fixed-target data, important discrepancies remain for the χ_{c1}/χ_{c2} production ratio and J/ψ (ψ') polarization. These discrepancies, as well as the differences between pion- and proton-induced collisions, emphasize the need for including higher twist effects in addition to the color octet mechanism. [S0556-2821(96)05515-4]

PACS number(s): 13.85.Ni, 13.88.+e, 14.40.Gx

Long-Distance Matrix Elements (LDMEs) PRD 54, 2005 (1996)

$$\langle \mathcal{O}_{1,8}^H [{}^{2S+1}L_J] \rangle$$

H	$q\bar{q}$	GG	qG
$J/\psi, \psi(2S)$	$\langle \mathcal{O}_8^H [{}^3S_1] \rangle (\mathcal{O}(\alpha_s^2))$	$\Delta_8^H (\mathcal{O}(\alpha_s^2))$ $\langle \mathcal{O}_1^H [{}^3S_1] \rangle (\mathcal{O}(\alpha_s^3))$	
χ_{c0}	$\langle \mathcal{O}_8^H [{}^3S_1] \rangle (\mathcal{O}(\alpha_s^2))$	$\langle \mathcal{O}_1^H [{}^3P_0] \rangle (\mathcal{O}(\alpha_s^2))$	
χ_{c1}	$\langle \mathcal{O}_8^H [{}^3S_1] \rangle (\mathcal{O}(\alpha_s^2))$	$\langle \mathcal{O}_1^H [{}^3P_1] \rangle (\mathcal{O}(\alpha_s^3))$	$\langle \mathcal{O}_1^H [{}^3P_1] \rangle (\mathcal{O}(\alpha_s^3))$
χ_{c2}	$\langle \mathcal{O}_8^H [{}^3S_1] \rangle (\mathcal{O}(\alpha_s^2))$	$\langle \mathcal{O}_1^H [{}^3P_2] \rangle (\mathcal{O}(\alpha_s^2))$	

$$\Delta_8^H = \langle \mathcal{O}_8^H [{}^1S_0] \rangle + \frac{3}{m_c^2} \langle \mathcal{O}_8^H [{}^3P_0] \rangle + \frac{4}{5m_c^2} \langle \mathcal{O}_8^H [{}^3P_2] \rangle$$

H	$\langle \mathcal{O}_1^H [{}^3S_1] \rangle$	$\langle \mathcal{O}_1^H [{}^3P_0] \rangle / m_c^2$	$\langle \mathcal{O}_8^H [{}^3S_1] \rangle$	Δ_8^H
J/ψ	1.16		6.6×10^{-3}	3×10^{-2}
$\psi(2S)$	0.76		4.6×10^{-3}	5.2×10^{-3}
χ_{c0}		0.044	3.2×10^{-3}	

color-singlet (CS) LDMEs

color-octet (CO) LDMEs

Determined by fit of proton- and pion-induced data

$$\sigma_{J/\psi} = \sigma_{J/\psi}^{direct} + Br(\psi(2S) \rightarrow J/\psi X) \sigma_{\psi(2S)} + \sum_{J=0}^2 Br(\chi_{cJ} \rightarrow J/\psi \gamma) \sigma_{\chi_{cJ}}$$

Jpsi and Psi(2S)

$$\text{LDME} \langle O_{1,8}^H [{}^{2S+1}L_J] \rangle$$

$$\hat{\sigma}(gg \rightarrow \psi') = \frac{5\pi^3 \alpha_s^2}{12(2m_c)^3 s} \delta(x_1 x_2 - 4m_c^2/s) \left[\langle O_8^{\psi'}({}^1S_0) \rangle + \frac{3}{m_c^2} \langle O_8^{\psi'}({}^3P_0) \rangle + \frac{4}{5m_c^2} \langle O_8^{\psi'}({}^3P_2) \rangle \right]$$

GG $+ \frac{20\pi^2 \alpha_s^3}{81(2m_c)^5} \Theta(x_1 x_2 - 4m_c^2/s) \langle O_1^{\psi'}({}^3S_1) \rangle z^2 \left[\frac{1-z^2+2z \ln z}{(1-z)^2} + \frac{1-z^2-2z \ln z}{(1+z)^3} \right],$ (4)

$$\hat{\sigma}(gq \rightarrow \psi') = 0, \quad (5)$$

q \bar{q} $\hat{\sigma}(q\bar{q} \rightarrow \psi') = \frac{16\pi^3 \alpha_s^2}{27(2m_c)^3 s} \delta(x_1 x_2 - 4m_c^2/s) \langle O_8^{\psi'}({}^3S_1) \rangle.$ (6)

Non-relativistic QCD model (NRQCD)

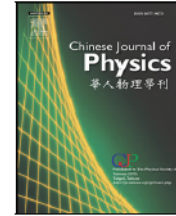
[Chin.J.Phys. 73 \(2021\) 13](#); [arXiv: 2103.11660](#)



Contents lists available at [ScienceDirect](#)

Chinese Journal of Physics

journal homepage: www.elsevier.com/locate/cjph



NRQCD analysis of charmonium production with pion and proton beams at fixed-target energies

Chia-Yu Hsieh ^{a,b,1}, Yu-Shiang Lian ^{a,c,1}, Wen-Chen Chang ^{a,*}, Jen-Chieh Peng ^d,
Stephane Platchkov ^e, Takahiro Sawada ^f

^a Institute of Physics, Academia Sinica, Taipei 11529, Taiwan

^b Department of Physics, National Central University, 300 Zhongda Road, Zhongli 32001, Taiwan

^c Department of Physics, National Kaohsiung Normal University, Kaohsiung County 824, Taiwan

^d Department of Physics, University of Illinois at Urbana-Champaign, Urbana, Illinois 61801, USA

^e IRFU, CEA, Université Paris-Saclay, 91191 Gif-sur-Yvette, France

^f Department of Physics, Osaka City University, Osaka 558-8585, Japan

ARTICLE INFO

Keywords:

Charmonium production

Pion PDFs

NRQCD

Color-octet matrix elements

Gluon

ABSTRACT

We present an analysis of hadroproduction of J/ψ and $\psi(2S)$ at fixed-target energies in the framework of non-relativistic QCD (NRQCD). Using both pion- and proton-induced data, a new determination of the color-octet long-distance matrix elements (LDMEs) is obtained. Compared with previous results, the contributions from the $q\bar{q}$ and color-octet processes are significantly enhanced, especially at lower energies. A good agreement between the pion-induced J/ψ production data and NRQCD calculations using the newly obtained LDMEs is achieved. We find that the pion-induced charmonium production data are sensitive to the gluon density of pions, and favor pion PDFs with relatively large gluon contents at large x .

Non-relativistic QCD model (NRQCD)

[Phys. Rev. D 107, 056008 \(2023\)](#); [arXiv: 2209.04072](#)

PHYSICAL REVIEW D **107**, 056008 (2023)

Fixed-target charmonium production and pion parton distributions

Wen-Chen Chang¹, Jen-Chieh Peng², Stephane Platchkov³, and Takahiro Sawada⁴

¹*Institute of Physics, Academia Sinica, Taipei 11529, Taiwan*

²*Department of Physics, University of Illinois at Urbana-Champaign, Urbana, Illinois 61801, USA*

³*IRFU, CEA, Université Paris-Saclay, 91191 Gif-sur-Yvette, France*

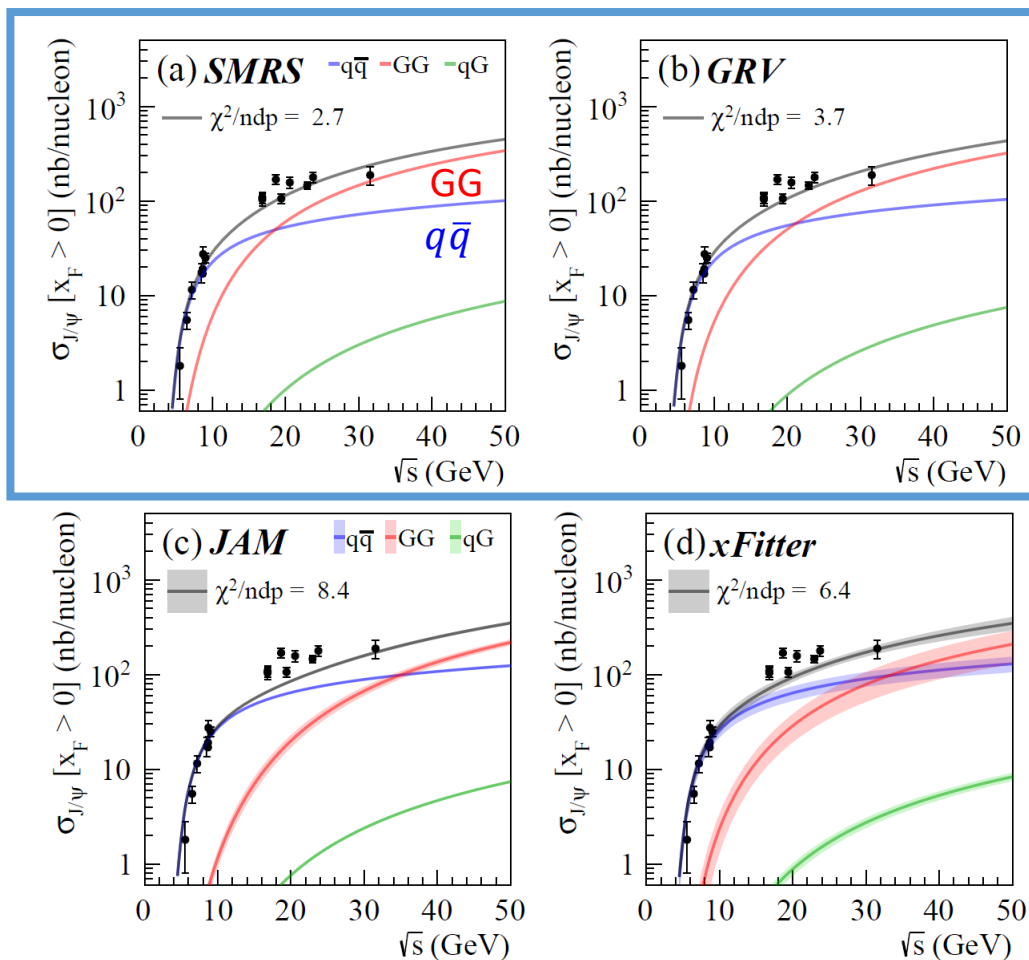
⁴*Nambu Yoichiro Institute of Theoretical and Experimental Physics, Osaka Metropolitan University, Osaka 558-8585, Japan*



(Received 8 September 2022; accepted 31 January 2023; published 7 March 2023)

We investigate how charmonium hadroproduction at fixed-target energies can be used to constrain the gluon distribution in pions. Using nonrelativistic QCD (NRQCD) formulation, the J/ψ and $\psi(2S)$ cross sections as a function of longitudinal momentum fraction x_F from pions and protons colliding with light targets, as well as the $\psi(2S)$ to J/ψ cross section ratios, are included in the analysis. The color-octet long-distance matrix elements are found to have a pronounced dependence on the pion parton distribution functions (PDFs). This study shows that the x_F differential cross sections of pion-induced charmonium production impose strong constraints on the pion's quark and gluon PDFs. In particular, the pion PDFs with larger gluon densities provide a significantly better description of the data. It is also found that the production of the $\psi(2S)$ state is associated with a larger quark-antiquark contribution, compared with J/ψ .

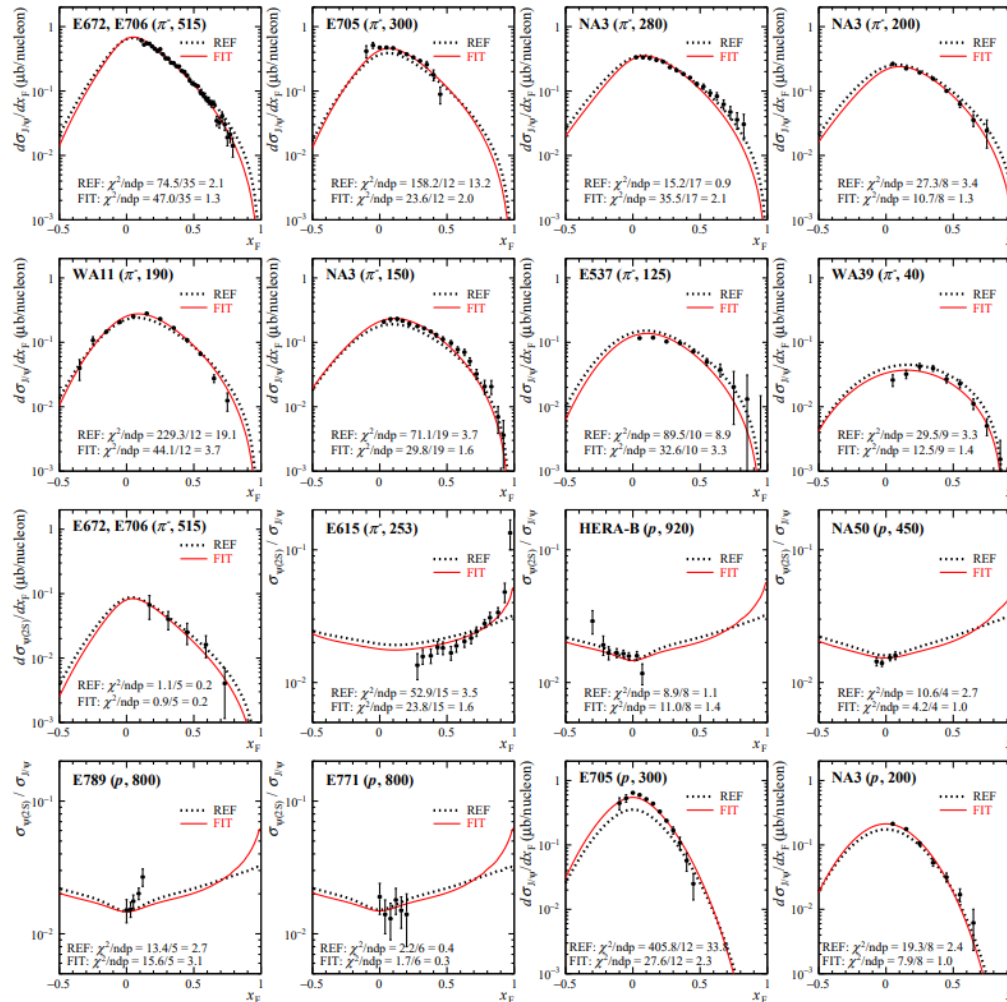
$\pi^- + N \rightarrow J\psi + X$: pion PDFs



Data favor SMRS and GRV PDFs with larger gluon densities at $x > 0.1$.

Data (Jpsi, psi') vs. NRQCD

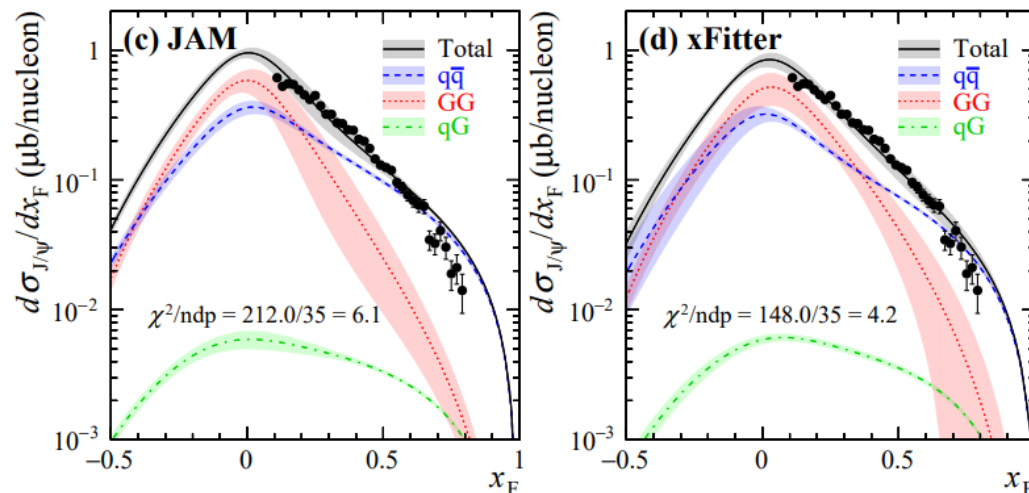
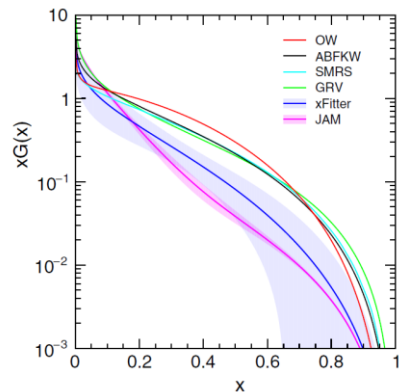
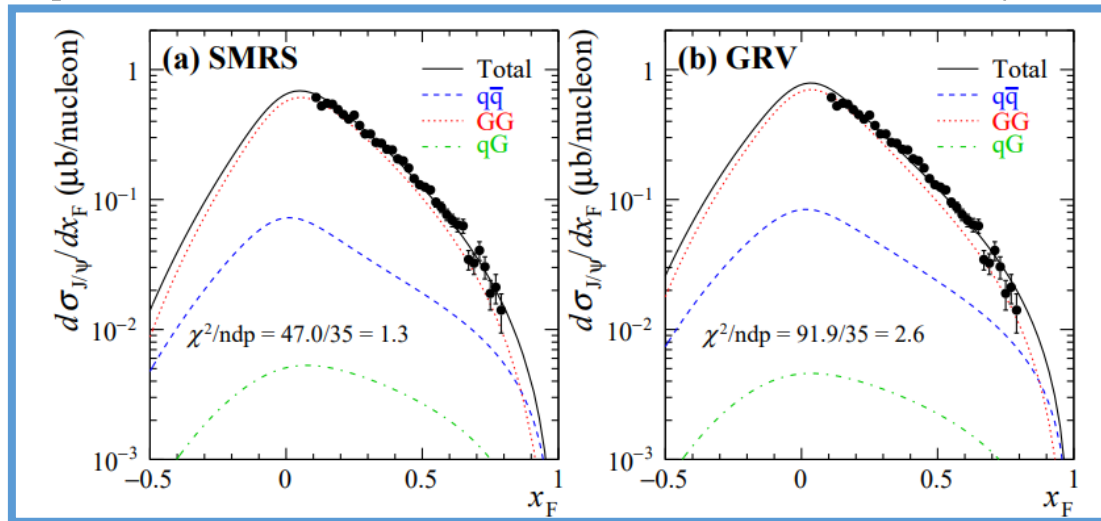
A common fit to both pion and proton induced data



We can achieve a reasonable description of the charmonium data with the proton and pion beams by NRQCD calculations with similar LDMEs obtained in Chin. J. Phys. 73 (2021) 13.

Data vs. NRQCD

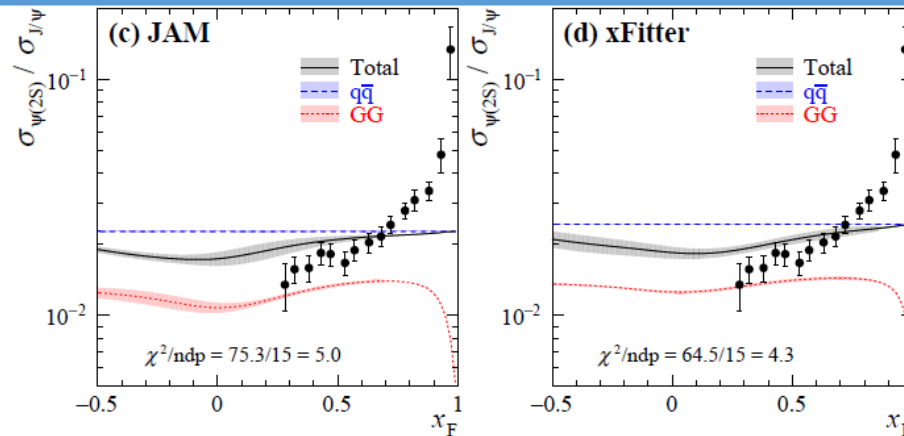
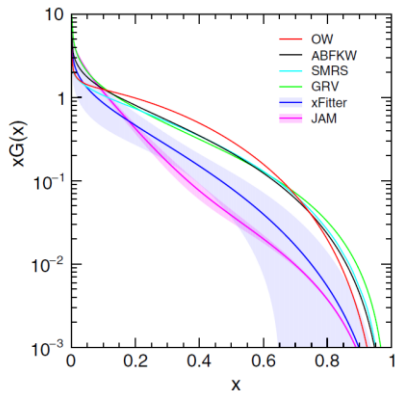
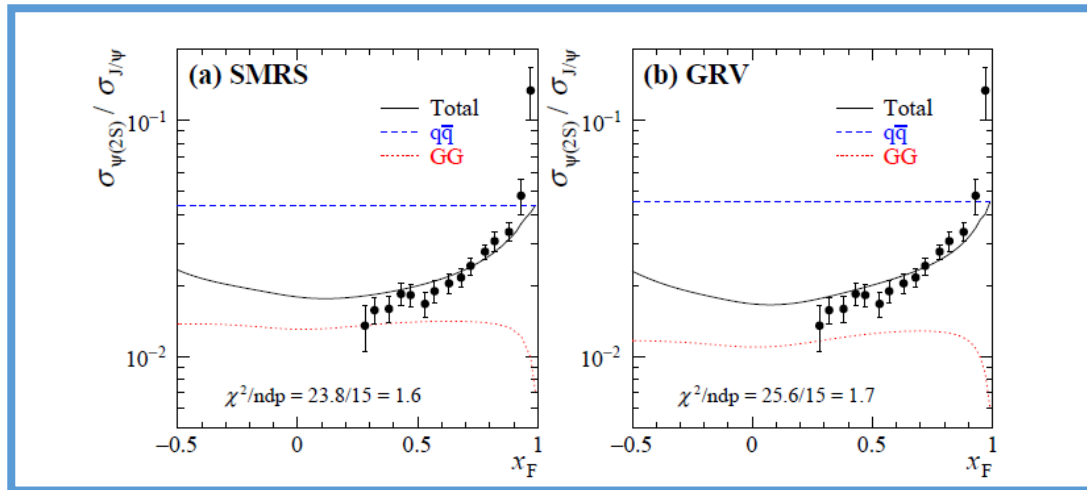
$[\pi^- + Be \rightarrow J\psi + X \text{ at } 515 \text{ GeV, PRD 53, 4723 (1996)}]$



Data favor SMRS and GRV PDFs with larger gluon densities at $x > 0.1$.

Data vs. NRQCD

$[\pi^- + W \rightarrow J\psi/\psi' + X \text{ at } 252 \text{ GeV, PRD 44, 1909 (1991)}]$



Data favor SMRS and GRV PDFs with larger gluon densities at $x > 0.1$.

Data vs. NRQCD Calculations

Data	SMRS		GRV		JAM		xFitter	
Exp	χ^2/ndp	F	χ^2/ndp	F	χ^2/ndp	F	χ^2/ndp	F
E672, E706 ($\sigma^{J/\psi}$)	1.3	0.80 ± 0.01	2.6	0.79 ± 0.01	6.1	1.14 ± 0.01	4.2	1.08 ± 0.02
E705 ($\sigma^{J/\psi}$)	2.0	0.98 ± 0.02	1.7	0.96 ± 0.02	4.1	1.19 ± 0.01	2.6	1.18 ± 0.01
NA3 ($\sigma^{J/\psi}$)	2.1	0.86 ± 0.02	2.3	0.87 ± 0.02	2.7	1.00 ± 0.02	2.9	1.01 ± 0.02
NA3 ($\sigma^{J/\psi}$)	1.3	0.87 ± 0.02	0.9	0.89 ± 0.02	1.8	0.92 ± 0.02	1.5	0.95 ± 0.02
WA11 ($\sigma^{J/\psi}$)	3.7	1.02 ± 0.02	8.5	1.02 ± 0.02	29.9	1.09 ± 0.01	22.0	1.12 ± 0.02
NA3 ($\sigma^{J/\psi}$)	1.6	1.24 ± 0.03	1.3	1.23 ± 0.03	1.5	1.10 ± 0.02	1.6	1.18 ± 0.03
E537 ($\sigma^{J/\psi}$)	3.3	0.88 ± 0.00	1.6	0.88 ± 0.01	2.6	0.88 ± 0.00	2.1	0.88 ± 0.01
WA39 ($\sigma^{J/\psi}$)	1.4	1.30 ± 0.04	1.4	1.18 ± 0.07	2.9	0.70 ± 0.00	1.3	0.70 ± 0.05
E672, E706 ($\sigma^{\psi(2S)}$)	0.2	0.80 ± 0.01	0.2	0.79 ± 0.01	0.3	1.14 ± 0.01	0.2	1.08 ± 0.02
E615 ($\sigma^{\psi(2S)}/\sigma^{J/\psi}$)	1.6	1 ± 0	1.7	1 ± 0	5.0	1 ± 0	4.3	1 ± 0
HERA-B ($\sigma^{\psi(2S)}/\sigma^{J/\psi}$)	1.4	1 ± 0	1.5	1 ± 0	1.2	1 ± 0	1.2	1 ± 0
NA50 ($\sigma^{\psi(2S)}/\sigma^{J/\psi}$)	1.0	1 ± 0	1.6	1 ± 0	1.3	1 ± 0	1.1	1 ± 0
E789 ($\sigma^{\psi(2S)}/\sigma^{J/\psi}$)	3.1	1 ± 0	3.3	1 ± 0	2.8	1 ± 0	2.9	1 ± 0
E771 ($\sigma^{\psi(2S)}/\sigma^{J/\psi}$)	0.3	1 ± 0	0.3	1 ± 0	0.3	1 ± 0	0.3	1 ± 0
E705 ($\sigma^{J/\psi}$)	2.3	1.20 ± 0.00	2.2	1.20 ± 0.00	5.7	1.20 ± 0.00	3.1	1.20 ± 0.00
NA3 ($\sigma^{J/\psi}$)	1.0	1.00 ± 0.01	1.2	1.00 ± 0.01	1.9	1.00 ± 0.01	1.6	1.00 ± 0.01

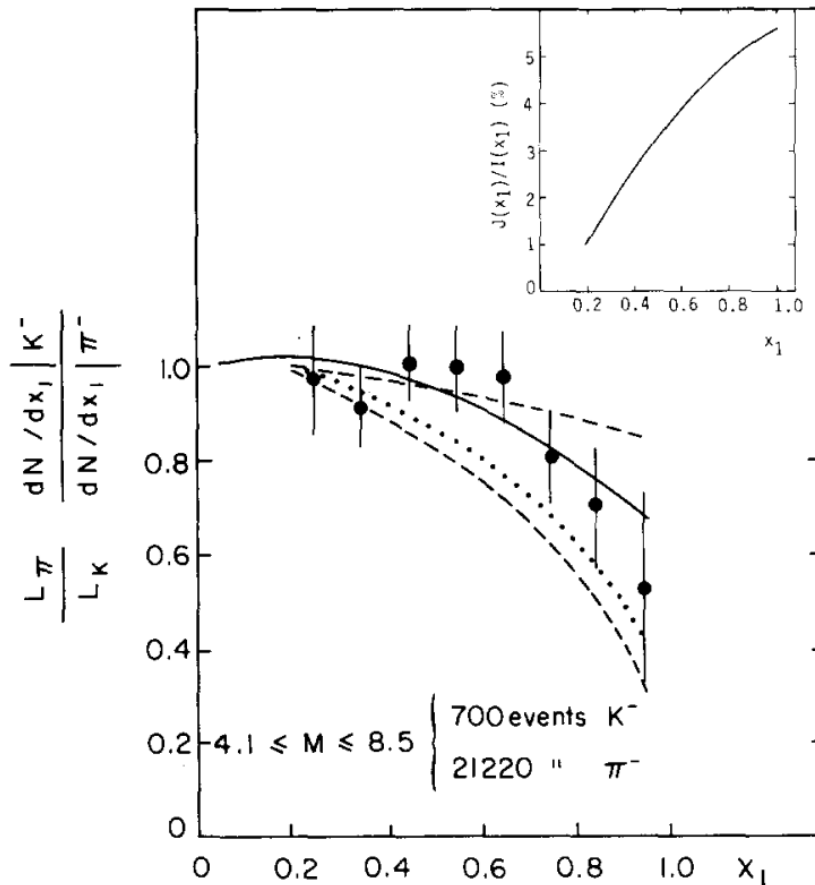
NRQCD calculations favor SMRS and GRV PDFs whose gluon densities at $x > 0.1$ are higher, compared with xFitter and JAM PDFs.

Kaon PDFs

Kaon/Pion Drell-Yan Ratios

NA10: J. Badier et al., Phys. Lett. B 93, 354 (1980)

$$\frac{\sigma^{DY}(K^-)}{\sigma^{DY}(\pi^-)}(x_F) = \frac{\bar{u}^K(x_1)u^N(x_2)}{\bar{u}^\pi(x_1)u^N(x_2)} = \frac{\bar{u}^K}{\bar{u}^\pi}(x_1)$$

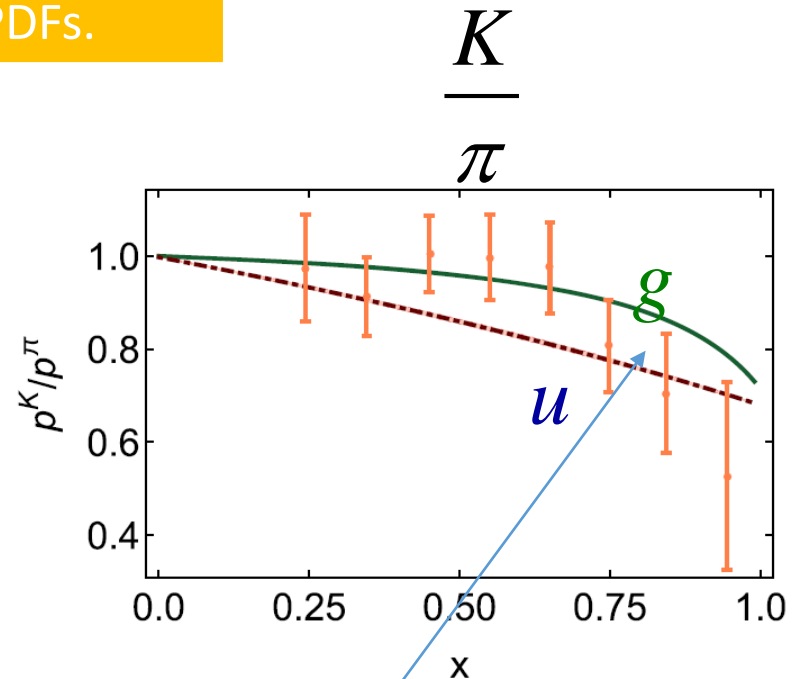
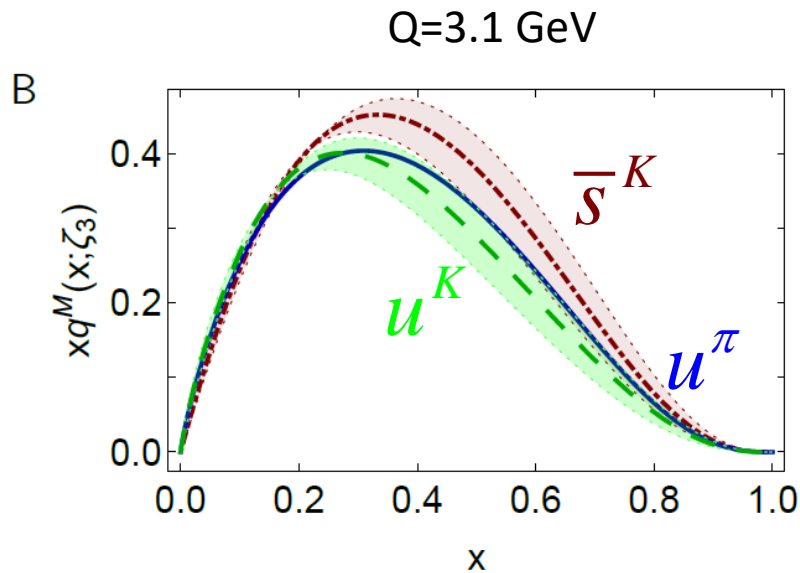


The \bar{u} distribution of kaon is softer than pion's.

Kaon PDFs: Dyson-Schwinger Equation (DSE)

[Eur. Phys. J. C \(2020\) 80:1064](#)

This paper contains comprehensive numerical information of determined kaon/pion PDFs.

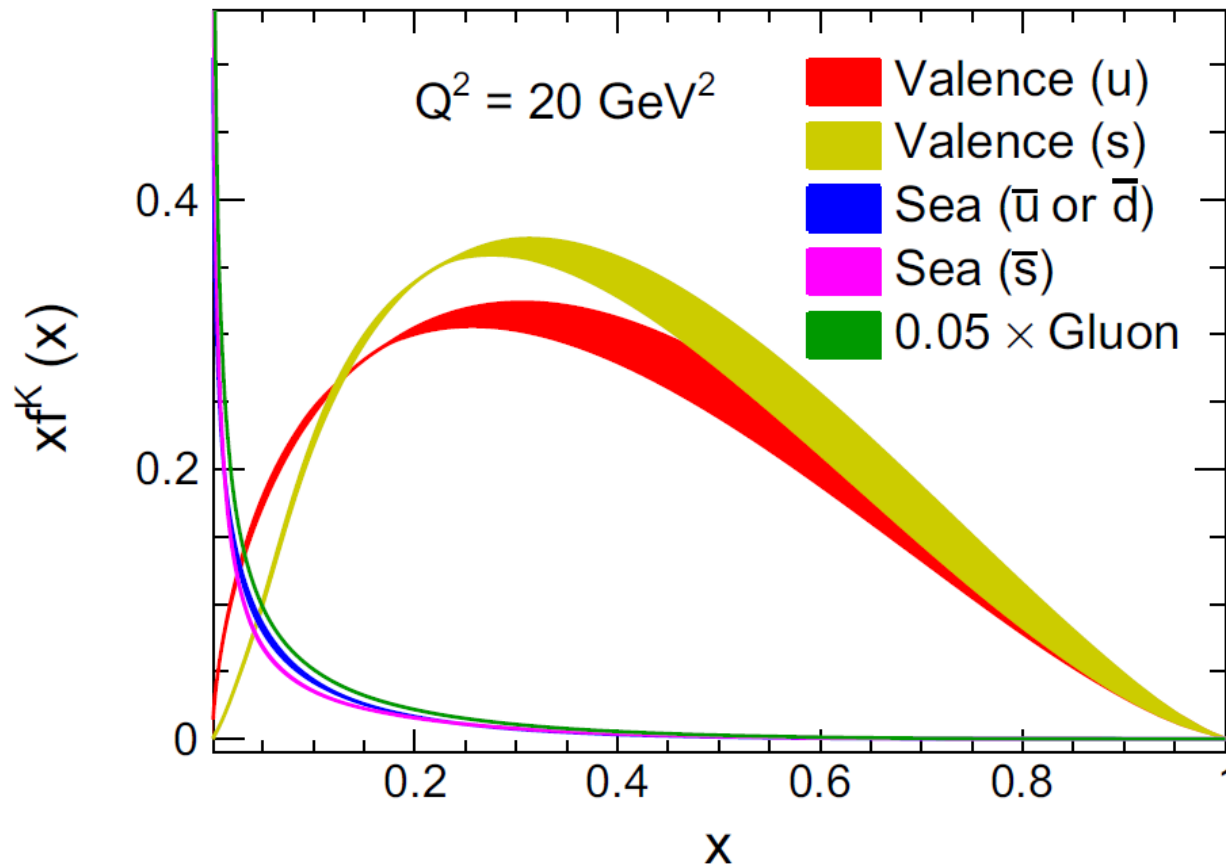


$$\langle x[2u^\pi(x; \zeta_3) + g^\pi(x; \zeta_3) + S^\pi(x; \zeta_3)] \rangle = 1.$$

A slightly smaller kaon gluon distribution at large x , compared to the pion.

Kaon PDFs: Maximum Entropy Input

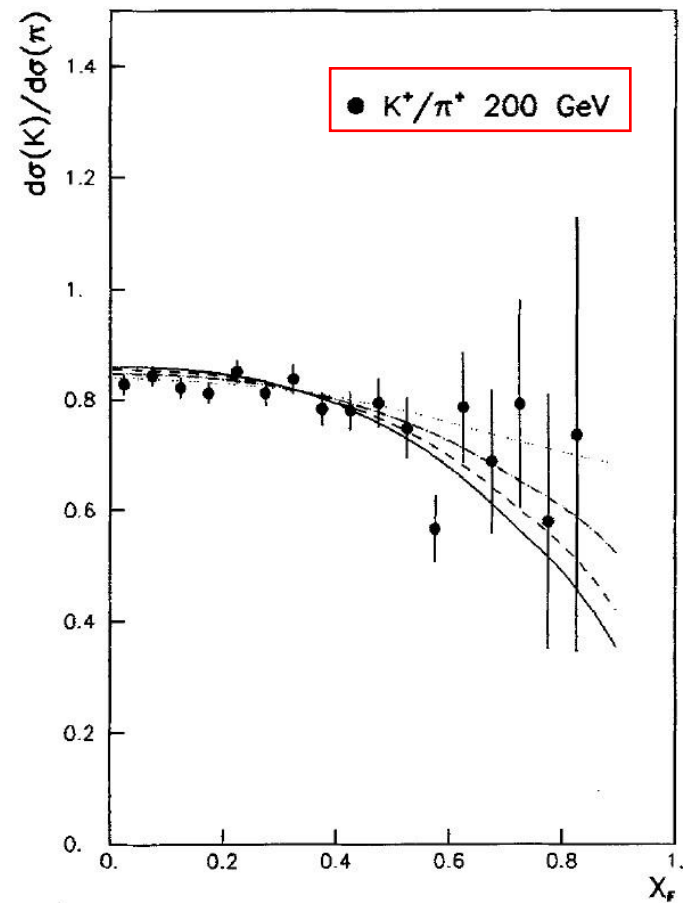
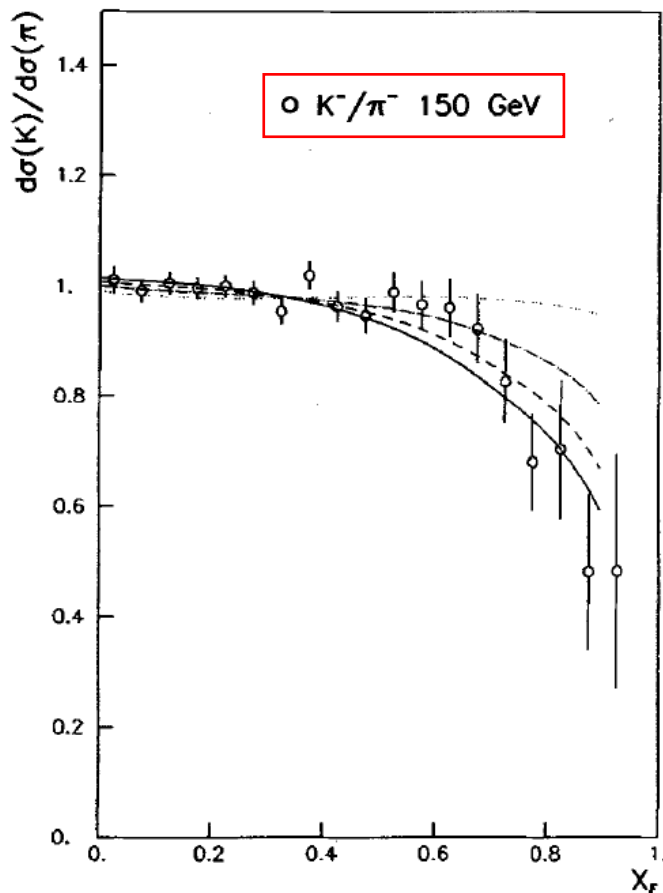
[Eur. Phys. J. C \(2021\) 81:302](#)



Kaon/Pion Jpsi Ratios

NA3: Z. Phys. C 20, 101 (1983)

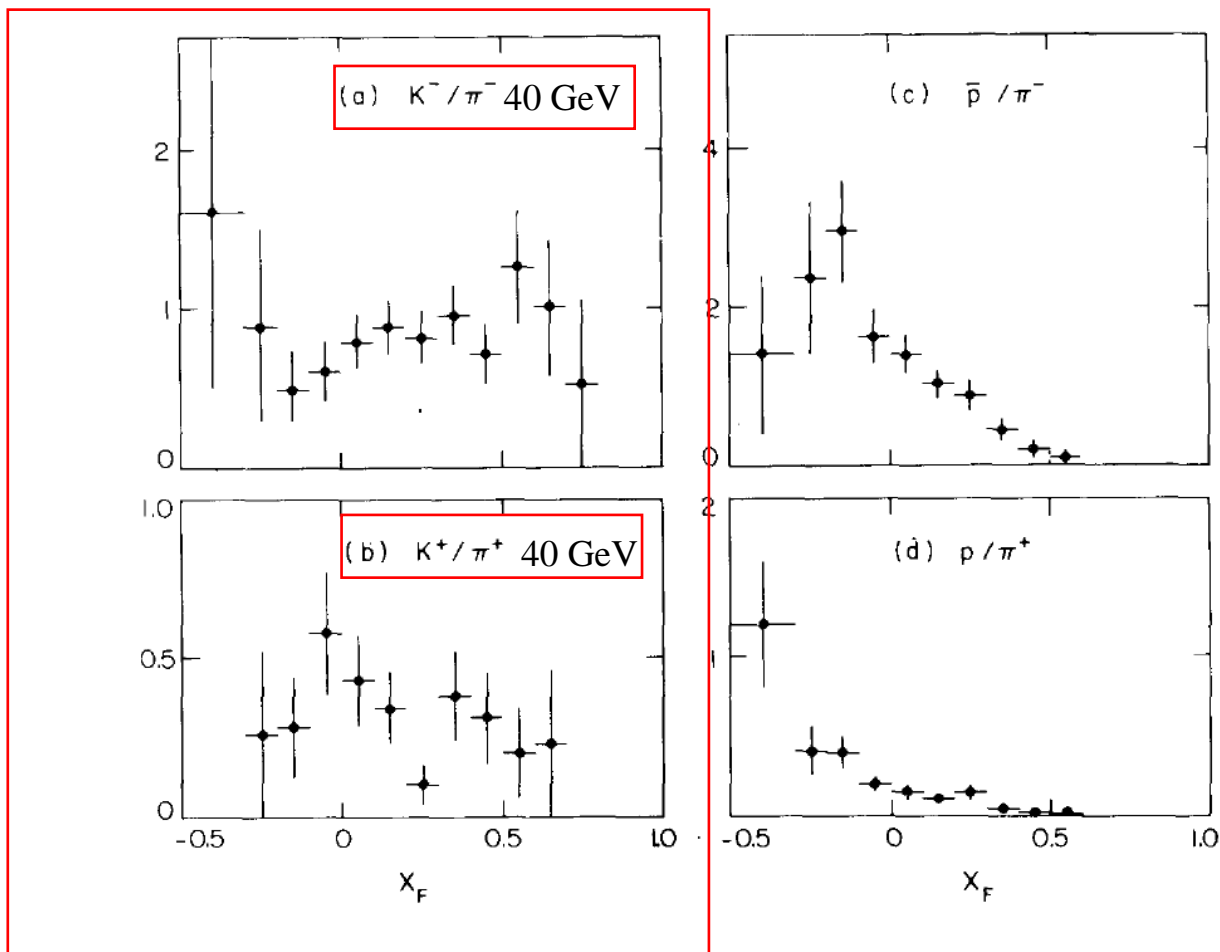
$$\frac{\sigma^{Jpsi}(K^-)}{\sigma^{Jpsi}(\pi^-)}(x_F) = \frac{\sigma(\bar{u}^K(x_1)u^N(x_2)) + \sigma(G^K(x_1)G^N(x_2))}{\sigma(\bar{u}^\pi(x_1)u^N(x_2)) + \sigma(G^\pi(x_1)G^N(x_2))} \quad \frac{\sigma^{Jpsi}(K^+)}{\sigma^{Jpsi}(\pi^+)}(x_F) = \frac{\sigma(u^K(x_1)\bar{u}^N(x_2)) + \sigma(\bar{s}^K(x_1)s^N(x_2)) + \sigma(G^K(x_1)G^N(x_2))}{\sigma(u^\pi(x_1)\bar{u}^N(x_2)) + \sigma(\bar{d}^\pi(x_1)d^N(x_2)) + \sigma(G^\pi(x_1)G^N(x_2))}$$



Kaon/Pion Jpsi Ratios

WA39: Phys. Lett. B 96, 411 (1980)

$$\frac{\sigma^{J\psi}(K^-)}{\sigma^{J\psi}(\pi^-)}(x_F) = \frac{\sigma(\bar{u}^K(x_1)u^N(x_2)) + \sigma(G^K(x_1)G^N(x_2))}{\sigma(\bar{u}^\pi(x_1)u^N(x_2)) + \sigma(G^\pi(x_1)G^N(x_2))} \quad \frac{\sigma^{J\psi}(K^+)}{\sigma^{J\psi}(\pi^+)}(x_F) = \frac{\sigma(u^K(x_1)\bar{u}^N(x_2)) + \sigma(\bar{s}^K(x_1)s^N(x_2)) + \sigma(G^K(x_1)G^N(x_2))}{\sigma(u^\pi(x_1)\bar{u}^N(x_2)) + \sigma(\bar{d}^\pi(x_1)d^N(x_2)) + \sigma(G^\pi(x_1)G^N(x_2))}$$



Kaon PDFs

[arXiv: 2402.02860](https://arxiv.org/abs/2402.02860)

Constraining kaon PDFs from Drell-Yan and J/ψ production

Wen-Chen Chang^{a,1}, Jen-Chieh Peng^{b,c,2}, Stephane Platchkov^{d,3}, Takahiro Sawada^{e,4}

^a*Institute of Physics, Academia Sinica, Taipei 11529, Taiwan*

^b*Department of Physics, University of Illinois at Urbana-Champaign, Urbana, Illinois 61801, USA*

^c*Department of Physics, National Central University, Chung-Li, 32001, Taiwan*

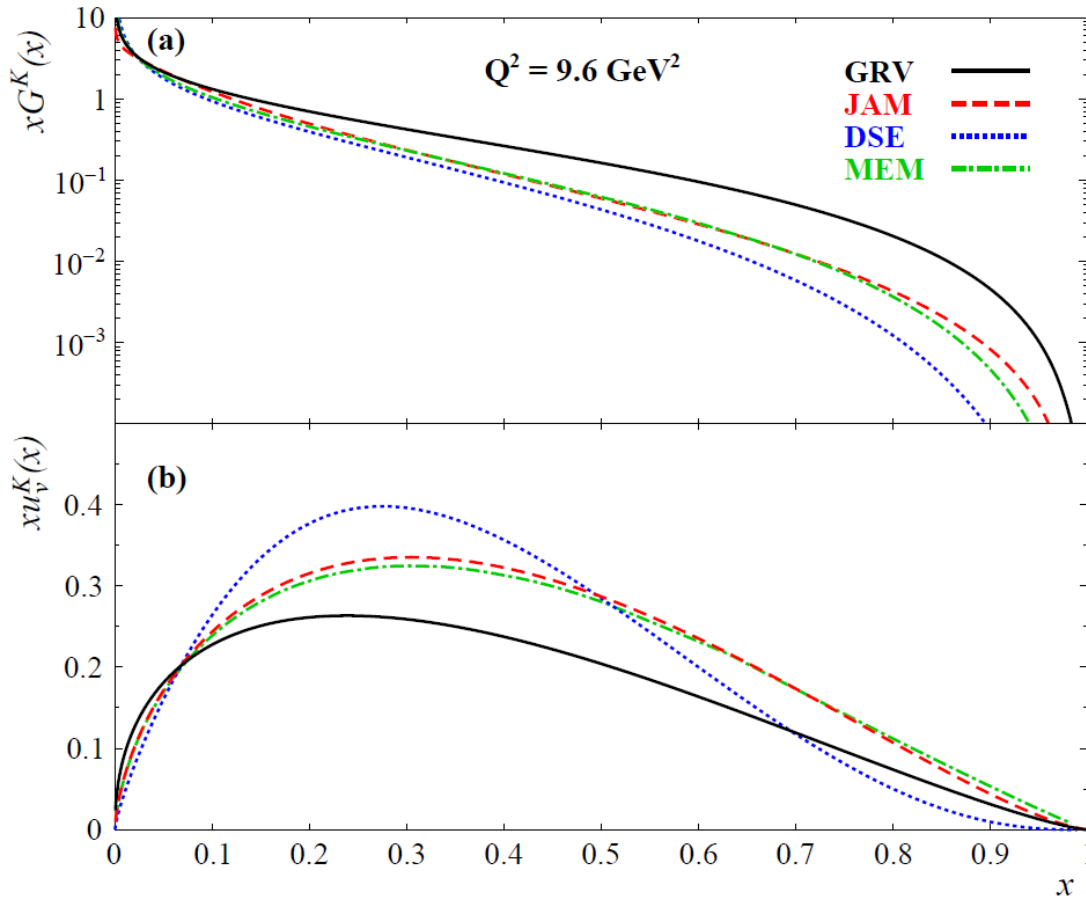
^d*IRFU, CEA, Université Paris-Saclay, 91191 Gif-sur-Yvette, France*

^e*Institute for Cosmic Ray Research, The University of Tokyo, Gifu 506-1205, Japan*

Abstract

The kaon parton distribution functions (PDFs) are poorly known due to paucity of kaon-induced Drell-Yan data. Nevertheless, these Drell-Yan data suggest a softer valence u quark distribution of kaon than that of pion. We discuss the opportunity to constrain kaon PDFs utilizing existing kaon-induced J/ψ production data. We compare the K^-/π^- and K^+/π^+ cross-section ratio data with calculations based on two global-fit parametrizations and two recent theoretical predictions for the kaon and pion PDFs, and test the results with two quarkonium production models. The K^-/π^- cross-section ratio for J/ψ production provides an independent evidence of different valence quark distributions in pion and kaon. The K^+/π^+ J/ψ data are found to be sensitive to the gluon distribution in kaon. We show that these J/ψ production data provide valuable constraints for evaluating the adequacy of currently available sets of kaon PDFs.

Kaon PDFs: GRV, JAM, DSE, MEM

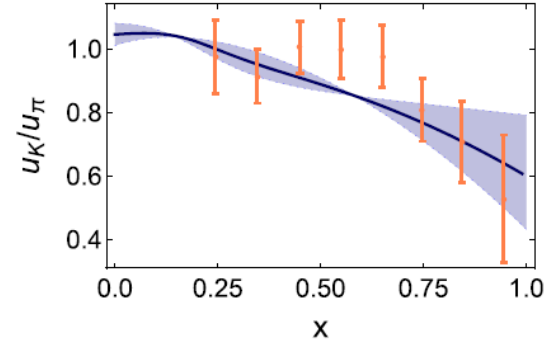


GRV, JAM: GRS ansatz

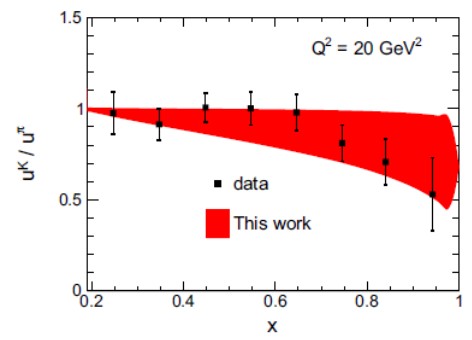
$$\bar{u}_v^K(x) = N_u \bar{u}_v^\pi(x)(1-x)^{0.17}$$

$$s_v^K(x) = 2\bar{u}_v^\pi(x) - \bar{u}_v^K(x)$$

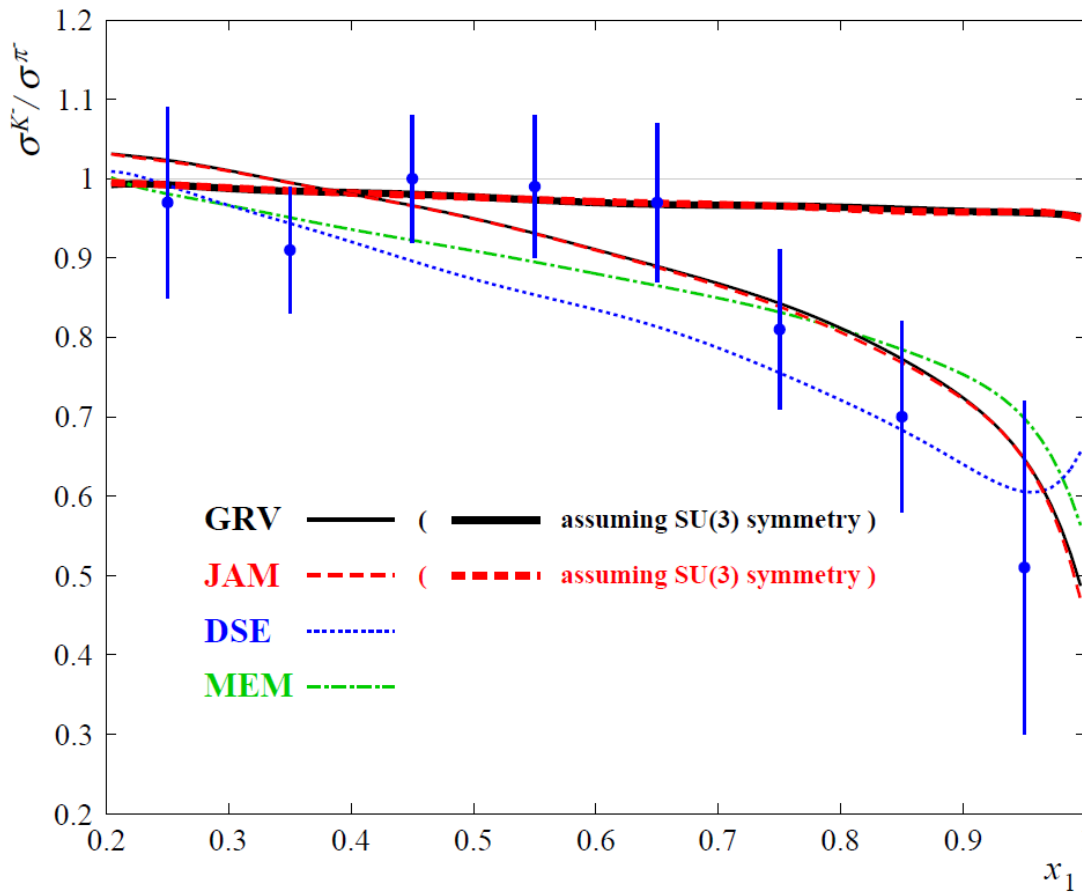
DSE: Eur. Phys. J. C (2020) 80:1064



MEM: Eur. Phys. J. C (2021) 81:302



K/pi Drell-Yan Ratios

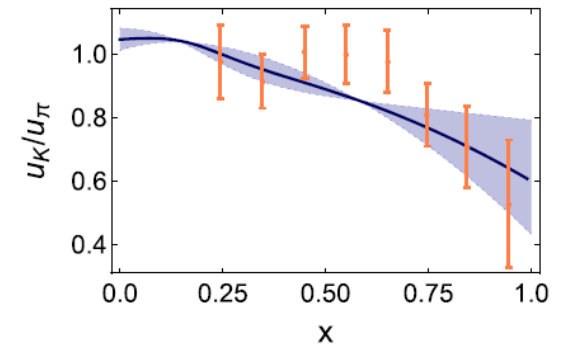


GRV, JAM: GRS ansatz

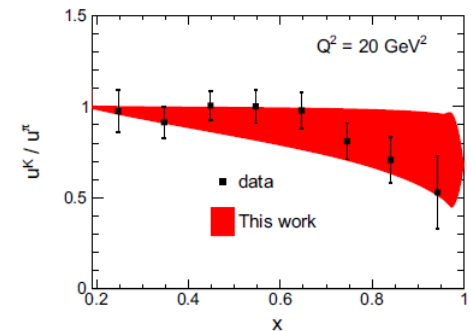
$$\bar{u}_v^K(x) = N_u \bar{u}_v^\pi(x) (1-x)^{0.17}$$

$$s_v^K(x) = 2\bar{u}_v^\pi(x) - \bar{u}_v^K(x)$$

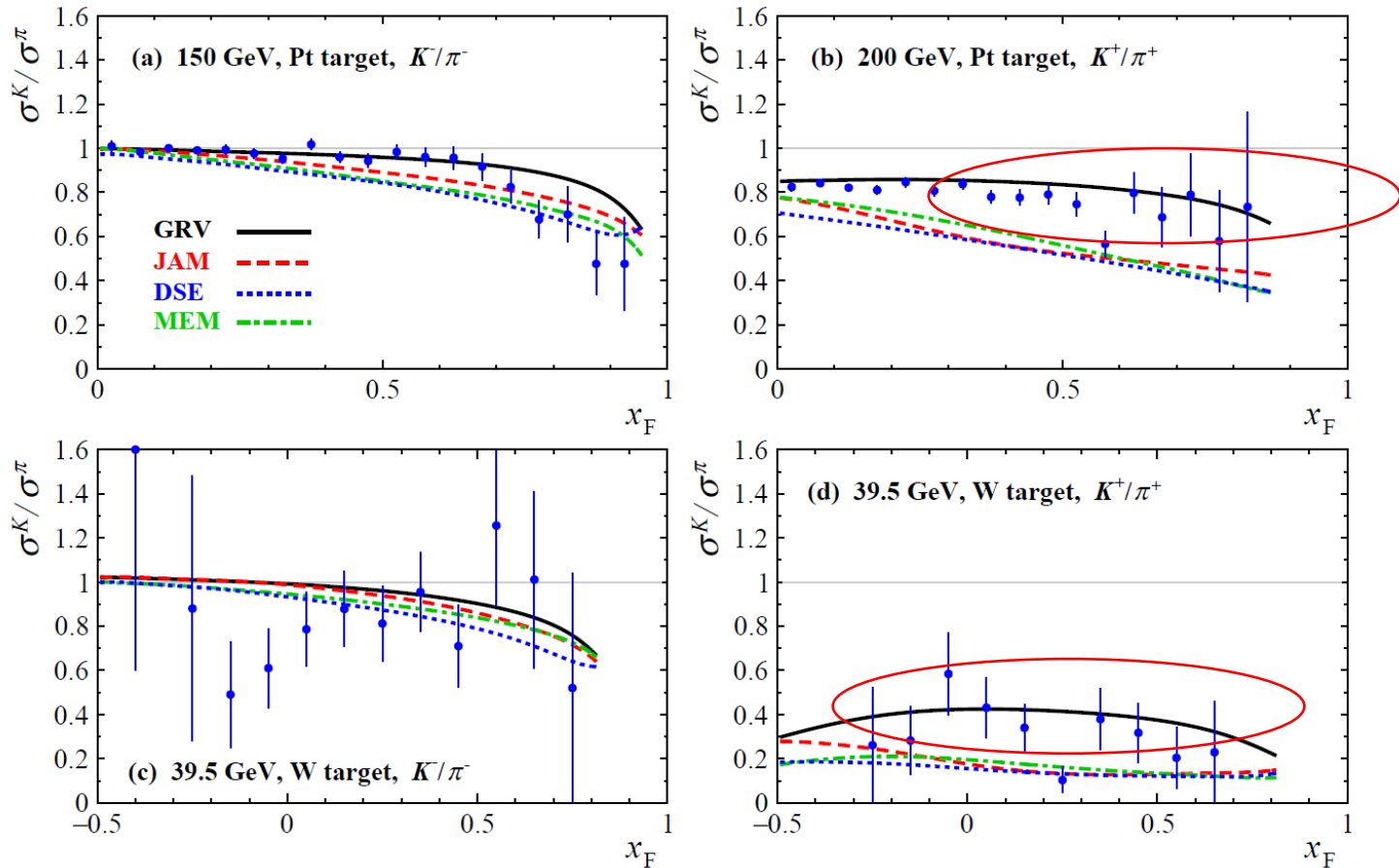
DSE: Eur. Phys. J. C (2020) 80:1064



MEM: Eur. Phys. J. C (2021) 81:302

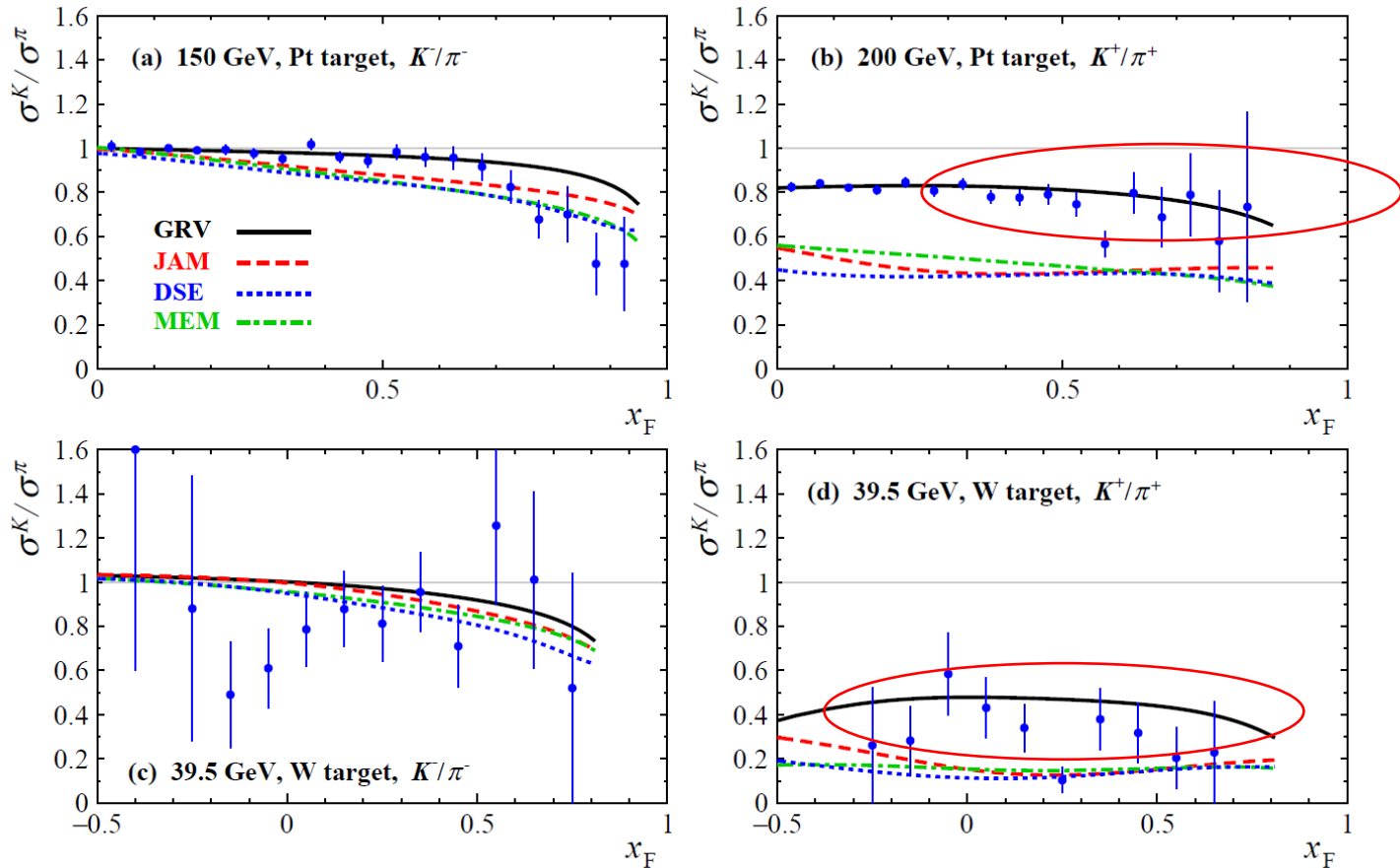


K/pi Jpsi Ratios: CEM



Data favor GRV PDFs with larger gluon densities at $x > 0.1$.

K/pi Jpsi Ratios: NRQCD



Data favor GRV PDFs with larger gluon densities at $x > 0.1$.

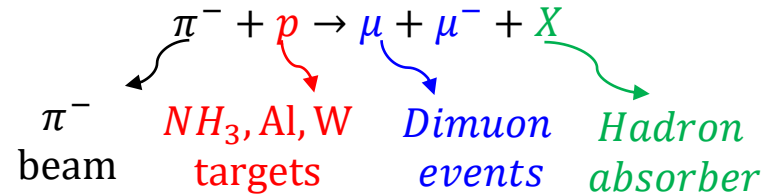
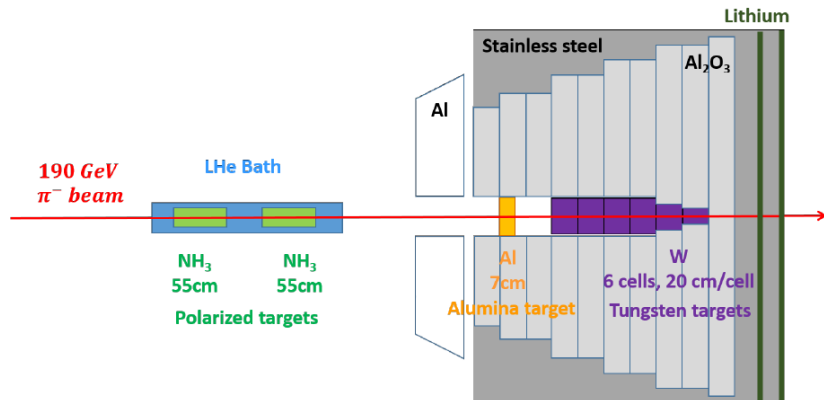
We need more data!

Outlook

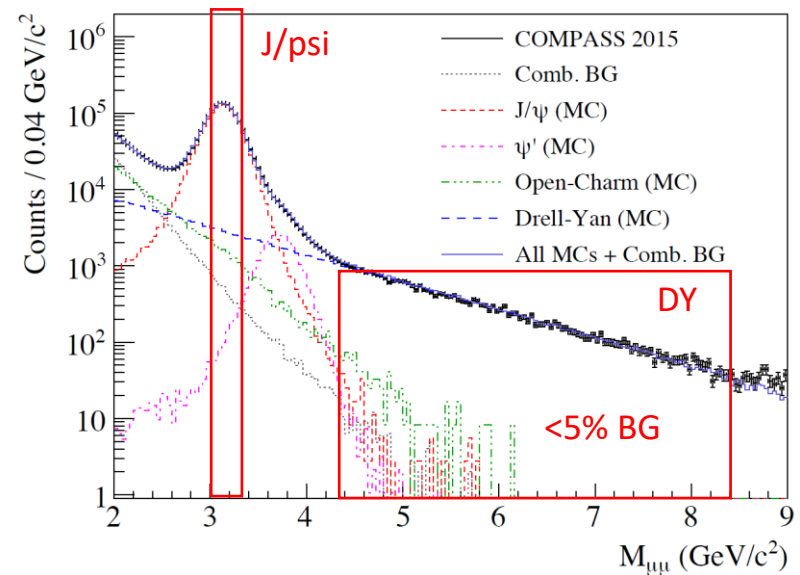
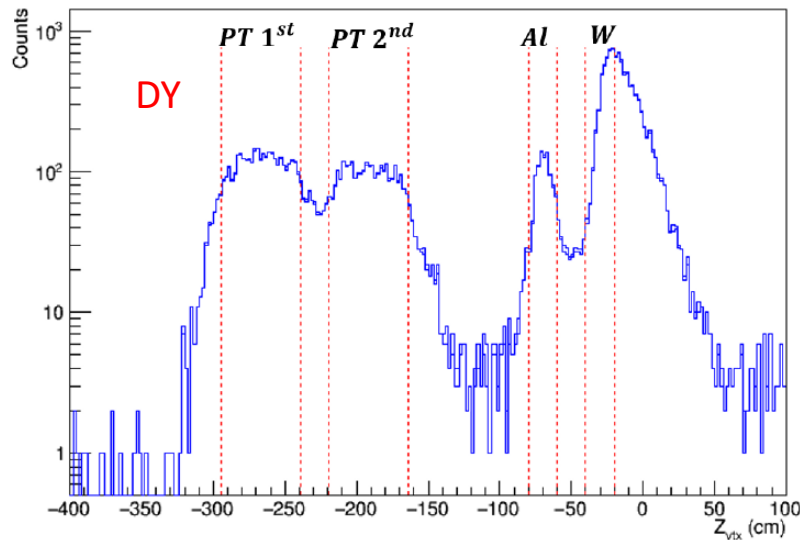
COMPASS

: π^- -induced DY/Jpsi

Catarina Quintans's Talk



- **Beam** : 190 GeV π^-
- **Target** : Polarized ammonia targets(PT), Al, W



AMBER

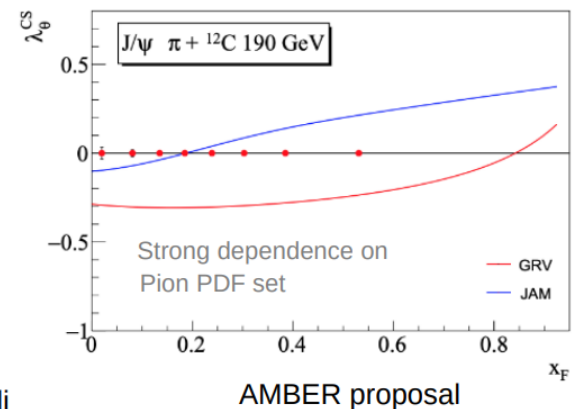
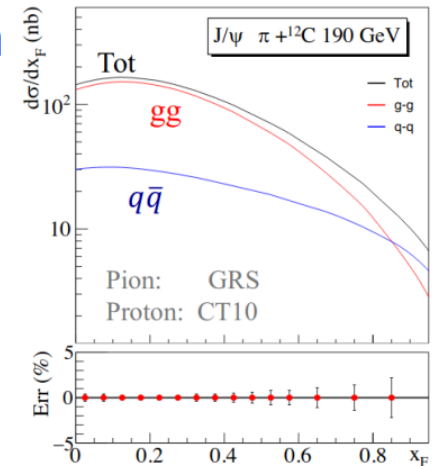
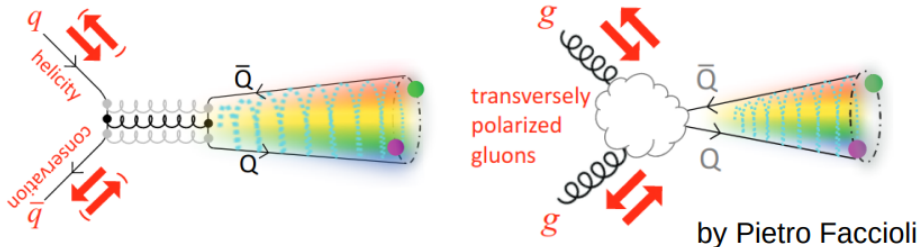
$:\pi^\pm / K^\pm$ -induced DY/Jpsi

Kun Liu's Talk



Phase-I: J/ψ & Gluon content in the pion

- Large statistics on J/ψ production at dimuon channel
- Inclusive: due to the hadron absorber, we cannot distinguish prompt production from the rest
- Expected significant feed-down: $\psi(2S)$, χ_{c1} , χ_{c2}
- In the low-pT regime
- Expected to have dominant contribution from $2 \rightarrow 1$ processes
- Use J/ψ polarization to distinguish production mechanism:



AMBER

: π^\pm / K^\pm -induced DY/Jpsi

Kun Liu's Talk



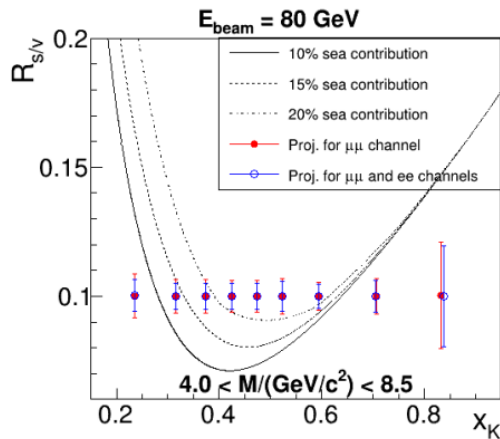
Phase-II: Kaon structure

Kaon structure: a window to the region of interference between the **Higgs mechanism** and the **EHM mechanism**

The only available experimental data:

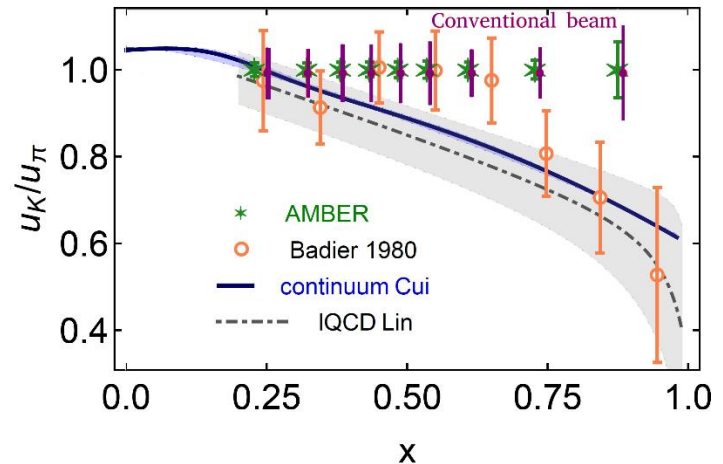
NA3 → 200 GeV K^- beam on 6 cm Pt target

↳ 700 kaon-induced Drell-Yan events



Kaon sea-valence separation using both charges kaon beams:

$$R_{s/v} = \frac{\sigma^{K^+C}}{\sigma^{K^-C} - \sigma^{K^+C}}$$



Assumed an RF-separated beam of 2×10^7 kaons/second.

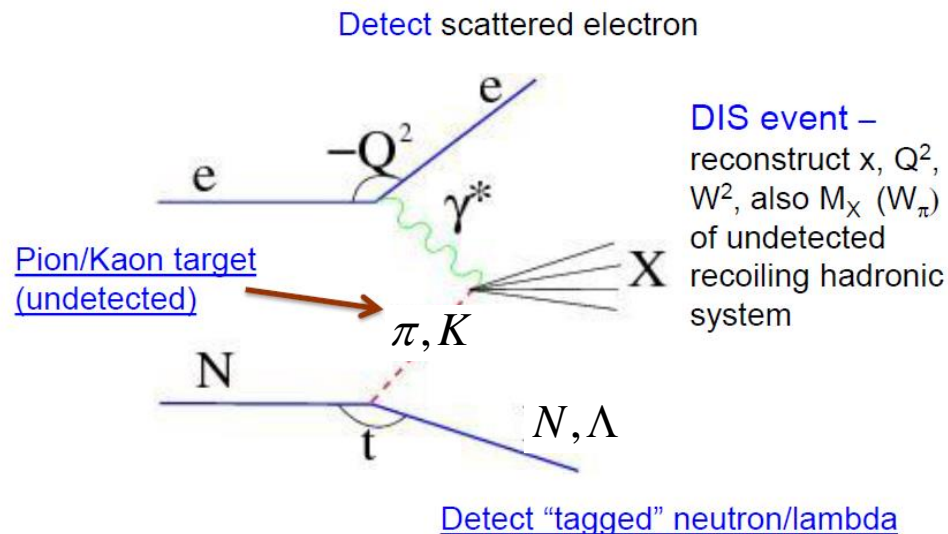
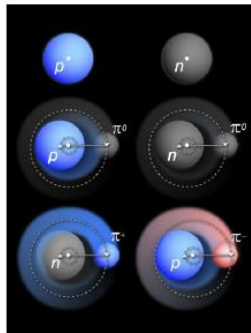
16

EIC: Tagged processes of DIS

Tanja Horn's Talk

Physics Objects for Pion/Kaon Structure Studies

- Sullivan process – scattering from nucleon-meson fluctuations



Summary

- Pion/kaon PDFs are the first step of their mass decomposition.
- Beside Drell-Yan, charmonium production provides valuable constraints for the pion/kaon PDFs.
- New COMPASS results of pion-induced DY/Jpsi
- Future AMBER results of π^\pm/K^\pm -induced DY/Jpsi
- Future measurements of Sullivan process in U.S. and China EIC